

THE ROLE OF MACROPHAGE SCAVENGER RECEPTOR IN ATHEROSCLEROSIS

THE ROLE OF MACROPHAGE SCAVENGER RECEPTOR CLASS B, TYPE I
(SR-BI) IN THE DEVELOPMENT OF ATHEROSCLEROSIS IN
APOLIPOPROTEIN E DEFICIENT MICE

By

Ali Amjad Rizvi, M.B.B.S., M.D.

A Thesis

Submitted to the School of Graduate Studies

in Partial Fulfillment of the Requirements

for the Degree of

Master of Science

McMaster University

© Copyright by Ali Amjad Rizvi, November 2003

**MASTER OF SCIENCE (2003)
(Biochemistry)**

**MCMASTER UNIVERSITY
Hamilton, Ontario**

TITLE: The Role of Macrophage Scavenger Receptor Class B,
Type I (SR-BI) in the Development of Atherosclerosis in
Apolipoprotein E Deficient Mice

AUTHOR: Ali Amjad Rizvi, M.B.B.S., M.D.

SUPERVISOR: Dr. Bernardo L. Trigatti

NUMBER OF PAGES: x, 92

Abstract

The high density lipoprotein (HDL) receptor Scavenger Receptor, Class B, Type I (SR-BI) is a 509 amino acid integral membrane protein which has been shown to have an important role in HDL-mediated reverse cholesterol transport. SR-BI has been shown to mediate selective uptake of cholesterol, and also mediates efflux of cholesterol to HDL as seen in in vitro cell culture studies. SR-BI is abundant in the liver and steroidogenic tissues, and is also present in macrophages, which play an important role in the initial stages of atherosclerotic development. SR-BI has been shown to be protective against atherosclerosis by way of overexpression and knockout (KO) studies in murine atherosclerosis models, including low density lipoprotein receptor (LDLR) knockout mice, apolipoprotein E (ApoE) knockout mice, and human apolipoprotein B (ApoB) transgenic mice. SR-BI/LDLR double knockout (dKO) mice show a 6-fold increase in diet-induced atherosclerosis compared to LDLR single KO controls, and SR-BI/ApoE dKO mice show severe coronary occlusion, myocardial infarction, and premature death on a normal chow diet. In both, plasma total cholesterol levels are significantly elevated, and associated with abnormally large HDL particles. The majority of SR-BI's atheroprotective effect has been shown to result from plasma cholesterol clearance by way of selective uptake in the liver. Recently, Covey et al showed that elimination of SR-BI expression in macrophages of LDLR KO mice resulted in increased diet-induced atherosclerosis. To see if SR-BI in macrophages contributes to the overall atheroprotective effect of SR-BI in ApoE KO mice, presumably by mediating cellular

cholesterol efflux to HDL, selective deletion of SR-BI was induced in bone marrow derived cells of ApoE KO mice using bone marrow transplantation. Female ApoE $-/-$ recipient mice were transplanted with either SR-BI $+/+$ ApoE $-/-$ or SR-BI $-/-$ ApoE $-/-$ bone marrow from male donor mice, and fed a high fat diet for 12 weeks. This resulted in significantly increased atherosclerosis in mice transplanted with SR-BI $-/-$ ApoE $-/-$ bone marrow, with a concomitant decrease in cholesterol associated with HDL-sized lipoproteins. No significant differences were seen in plasma total cholesterol levels or levels of cholesterol associated with non-HDL lipoproteins. These data suggest that SR-BI in macrophages contributes to SR-BI's overall protective effect against atherosclerosis, and also plays a role in the regulation of HDL cholesterol, in ApoE deficient mice.

ACKNOWLEDGMENTS

I would like to thank my supervisor, Dr. Bernardo Trigatti, for allowing me the opportunity, guidance, and resources to pursue graduate studies in his laboratory. I would also like to thank Scott Covey for sharing his experience, guidance, and support during the course of my study, and Danny Wang for his technical help and assistance during my project. Additionally, I am grateful to my committee members Dr. David Andrews and Dr. Suleiman Igdoura for their guidance during the course of my work.

I would also like to thank all the members of Dr. Trigatti's laboratory, especially Ayesha Ahmed, Tom Baumgartner, Judy Lin, Katie Chan, Jevon Clement, Shephali Gandhi, and Vivienne Tedesco for their friendship and for making the lab atmosphere enjoyable, vibrant, and stimulating.

Finally, I would like to thank my parents, Dr. Amjad and Dr. Nayyer Rizvi, my sister, Dr. Tara Rizvi, and my brothers Hussain and Zameer for time, space, and environment.

Table of Contents

List of Figures	viii
List of Tables	ix
List of Abbreviations	x
1. Introduction	1
1.1 Atherosclerosis and Plasma Cholesterol	1
1.2 Scavenger Receptor, Class B, Type I and Selective Uptake	5
1.3 Role of SR-BI in Various Physiological Systems	9
1.3.1 Role of SR-BI in Lipoprotein Metabolism	9
1.3.2 Role of SR-BI in Cardiovascular Pathology	12
1.3.3 Role of SR-BI in the Female Reproductive System	14
1.3.4 Role of SR-BI in the Gastrointestinal System	15
1.3.5 Effects of SR-BI on Erythrocyte Morphology	16
1.4 Macrophage SR-BI and Bone Marrow Transplantation	20
1.5 Project Overview	23
1.6 Hypothesis	24
2. Materials and Methods	25
2.1 Materials	25
2.2 Methods	27
2.2.1 Generation and Maintenance of Mice	27
2.2.2 Preparation of DNA from Mouse Tail Biopsies	28
2.2.3 Collection of Blood	29

2.2.4	Preparation of Plasma and Analysis of Plasma and Lipoprotein Cholesterol	30
2.2.5	Bone Marrow Transplantation	32
2.2.6	Induction of Atherosclerosis	34
2.2.7	Preparation of Blood Cell DNA	35
2.2.8	Flow Cytometric Analysis of Blood Cells	35
2.2.9	PCR Genotyping	37
2.2.10	Tissue Collection and Morphometric Analysis of Aortas and Aortic Sinus	39
3.	Results	43
3.1	Conditions for Bone Marrow Transplantation and Repopulation	43
3.2	PCR to Test for Repopulation	52
3.3	Analysis of Plasma Cholesterol Levels and Lipoprotein Profiles	55
3.4	Histological Assessment of Atherosclerosis Development	64
3.5	Effects of Selective Lack of SR-BI in Bone Marrow Derived Cells on Lipoprotein and Cholesterol Metabolism and Atherosclerosis in ApoE ^{-/-} Mice	75
4.	Discussion	76
4.1	Potential Mechanisms by which SR-BI may Protect Against Atherosclerosis	76
4.2	Effects of SR-BI Deletion in Bone Marrow Derived Cells on Lipoprotein Metabolism in ApoE Knockout Mice	78
4.3	Effects of SR-BI Deletion in Bone Marrow Derived Cells on Atherosclerosis in ApoE Knockout Mice	81
5.	References	84

List of Figures

Figure 1. Flow cytometric analysis of GFP and CD11b expression in blood cells.	46
Figure 2. Flow cytometric analysis of blood cells after bone marrow transplantation.	48
Figure 3. Effect of radiation dose on bone marrow repopulation.	50
Figure 4. PCR genotyping analysis of blood cells after bone marrow transplantation for repopulation assessment.	54
Figure 5. Plasma total cholesterol in ApoE ^{-/-} mice transplanted with SR-BI ^{+/+} ApoE ^{-/-} (black) or SR-BI ^{-/-} ApoE ^{-/-} (white) bone marrow.	59
Figure 6. Comparison of plasma lipoprotein profiles 16 weeks post-transplantation in mice that received SR-BI ^{+/+} ApoE ^{-/-} (closed circles) or SR-BI ^{-/-} ApoE ^{-/-} (open circles) bone marrow, fed a normal chow (A) or a high fat diet (B).	60
Figure 7. Plasma total cholesterol associated with VLDL-sized lipoproteins in ApoE ^{-/-} mice transplanted with SR-BI ^{+/+} ApoE ^{-/-} (black) or SR-BI ^{-/-} ApoE ^{-/-} (white) bone marrow.	61
Figure 8. Plasma total cholesterol associated with IDL/LDL-sized lipoproteins in ApoE ^{-/-} mice transplanted with SR-BI ^{+/+} ApoE ^{-/-} (black) or SR-BI ^{-/-} ApoE ^{-/-} (white) bone marrow.	62
Figure 9. Plasma total cholesterol associated with HDL-sized lipoproteins in ApoE ^{-/-} mice transplanted with SR-BI ^{+/+} ApoE ^{-/-} (black) or SR-BI ^{-/-} ApoE ^{-/-} (white) bone marrow.	63
Figure 10. Atherosclerosis in aortas from bone marrow transplanted mice.	66
Figure 11. Extent of atherosclerosis in aortas from bone marrow transplanted mice.	67
Figure 12. Extent of atherosclerosis in the thoracic aorta from bone marrow transplanted mice.	68
Figure 13. Extent of atherosclerosis in abdominal aortas from bone marrow transplanted mice.	69

Figure 14. Histological analysis of atherosclerotic plaque in the aortic roots of bone marrow transplanted mice.	72
Figure 15. Cross sectional area of atherosclerotic plaque in the aortic roots from ApoE ^{-/-} mice transplanted with bone marrow from either SR-BI ^{+/+} ApoE ^{-/-} or SR-BI ^{-/-} ApoE ^{-/-} bone marrow.	73
Figure 16. Cross sectional area of atherosclerotic plaque in the aortic sinus.	74

List of Tables

Table 1. Effects of SR-BI manipulation on plasma lipoprotein cholesterol levels and atherosclerosis in mice with various genetic manipulations.	18
Table 2. Reagents and Suppliers	25
Table 3. Coupled enzymatic assay (Infinity Cholesterol Liquid Stable Reagent Kit) kinetics.	31
Table 4. PCR reaction composition per 20 µl aliquot.	38
Table 5. Flow cytometric analysis of blood cells from non-transgenic and GFP-transgenic mice.	47
Table 6. Effect of radiation dose on bone marrow repopulation.	51

List of Abbreviations

ABCA1	ATP Binding Cassette Transporter I
ACAT	Acyl-CoA Cholesterol Acyl Transferase
AcLDL	Acetylated Low Density Lipoprotein
ApoAI	Apolipoprotein AI
ApoAII	Apolipoprotein AII
ApoB	Apolipoprotein B
ApoE	Apolipoprotein E
CETP	Cholesterol Ester Transfer Protein
CHO	Chinese Hamster Ovary
FACS	Fluorescence Activated Cell Sorting
GFP	Green Fluorescent Protein
HDL	High Density Lipoprotein
IDL	Intermediate Density Lipoprotein
LCAT	Lecithin Cholesterol Acyl Transferase
LDL	Low Density Lipoprotein
mSR-BI	Murine Scavenger Receptor, Class B, Type I
SR-BI	Scavenger Receptor, Class B, Type I
SR-Biatt	Scavenger Receptor, Class B, Type I Attenuated
VLDL	Very Low Density Lipoprotein

1. Introduction

1.1 Atherosclerosis and Plasma Cholesterol

Atherosclerosis, the leading cause of death in North America, is characterized by deposition of lipid and fibrosis in artery walls, and is a major risk factor for stroke, heart disease, and vascular disease [Mahley RW, 1983]. Atherosclerosis is currently viewed as an inflammatory process instrumental in initiating and promoting plaque lesion development eventually resulting in thrombotic events [Libby P, 2003].

Hypercholesterolemia is a significant risk factor for the development of atherosclerosis. This link between elevated plasma cholesterol levels and atherosclerosis was first described a century ago when atherosclerosis was relatively uncommon [La Rosa JC, 2003]. Prevalence of atherosclerosis and coronary heart disease increased thereon as a result of factors such as cigarette smoking, high-fat diets, and sedentary lifestyles [La Rosa JC, 2003].

Cholesterol is primarily transported in blood via lipoproteins, including low density lipoproteins (LDL) and high density lipoproteins (HDL) [Libby P *et al*, 2001]. After being absorbed in the digestive system, cholesterol is packaged into chylomicrons, which are transported to the liver; chylomicrons mainly transport dietary triglycerides to extrahepatic tissues such as adipose tissue and muscles [Gotto AM Jr, 1988]. Cholesterol and remaining triglycerides are then transported to the liver, and chylomicron remnants are endocytosed and internalized into hepatic cells [Gotto AM Jr, 1988]. From the liver,

cholesterol is packaged into very low density lipoproteins (VLDL) and sent into circulation; VLDL also mainly consists of triglycerides, which is transported from the liver to extrahepatic tissues [Tulenko TN *et al*, 2002]. Lipoprotein lipase converts VLDL to LDL, by first hydrolyzing triglycerides, resulting in the generation of intermediate density lipoprotein (IDL), which is then converted to LDL [Tulenko TN *et al*, 2002]. LDL and HDL differ from chylomicrons and VLDL in that they are both composed of a hydrophobic core of cholesteryl esters, with a much smaller triglyceride component [Krieger M, 1998]. LDL is the major lipoprotein involved in the transport of cholesterol to peripheral tissues, whereas HDL is involved in a process called reverse cholesterol transport, mediating delivery of cholesterol from peripheral tissues back to the liver and steroidogenic tissues for metabolism, excretion, or steroid biosynthesis [Krieger M, 1998].

Unlike chylomicrons and VLDL, which are composed mainly of triglycerides, both LDL and HDL consist of an outer layer of phospholipid and free cholesterol surrounding a central hydrophobic core of cholesteryl esters [Krieger M, 1998]. Various apolipoproteins are associated with HDL and LDL. For instance, apolipoprotein AI (ApoAI) and apolipoprotein AII (ApoAII) are associated with HDL and are required for structural integrity as well as for the activity of enzymes such as lecithin cholesterol acyltransferase (LCAT), involved in cholesteryl ester synthesis, described later [Tailleux A, 2002]. Apolipoprotein B100 (ApoB100) is the only lipoprotein associated with LDL, playing an important function in binding to the LDL receptor [Krieger M, 1998].

The atherosclerotic process begins with endothelial injury and the accumulation of cholesterol (in the form of lipoproteins such as LDL) in the subendothelial region of the artery known as the intima [de Villiers WJ *et al*, 1999]. Oxidation of LDL, along with a variety of other factors, triggers monocytic invasion of the site. As the monocytes differentiate into macrophages, endocytosis of oxidized LDL occurs, and the intracellular accumulation of cholesterol results in the formation of foam cells, resulting in a fatty streak [Schwartz CJ *et al*, 1991; de Villiers WJ *et al*, 1999]. This is followed by smooth muscle cell migration and proliferation and the subsequent formation of an atherosclerotic plaque. As the lesion progresses, plaque rupture or thrombus formation may occur, potentially resulting in complete occlusion of the vessel and distal infarction [Schwartz CJ *et al*, 1991; de Villiers WJ *et al*, 1999].

The discovery of the LDL receptor by Brown and Goldstein in 1985 was a major contribution in the effort to partially understand the metabolic bases for vascular disease. Later, the Framingham Heart Study provided epidemiological evidence for a low plasma HDL level being an independent predictor for coronary artery disease development [Gordon T *et al*, 1977], meaning that plasma levels of plasma low density lipoprotein (LDL) cholesterol are directly related to the risk of developing atherosclerosis, whereas levels of plasma high density lipoprotein (HDL) cholesterol are inversely related to this risk [Krieger M, 1998; Kwiterovich PO Jr, 1998]. This is now known to be because of the role of HDL in reverse cholesterol transport.

Reverse cholesterol transport is the primary physiological process that protects peripheral tissues, such as macrophages in atherosclerotic plaque in the artery wall, from

excessive cholesterol accumulation [Krieger M, 2001; Tall AR, 1998]. This process is largely HDL mediated [Rigotti A *et al*, 1997]. The protein ABCA1 (ATP binding cassette transporter A1) mediates efflux of cholesterol from macrophages to ApoAI [Singaraja RR *et al*, 2003], a major apolipoprotein associated with HDL. Esterification of cholesterol is carried out by LCAT; from here, cholesteryl esters can be shuttled to other lipoproteins such as VLDL and LDL via cholesteryl ester transfer protein (CETP) [Yamashita S *et al*, 2001]. Any remaining HDL associated cholesteryl esters are taken up in the liver by a process known as selective lipid uptake [Glass C *et al*, 1983; see *1.2 Scavenger Receptor, Class B, Type I and Selective Uptake*]. Although most current atherosclerosis treatments revolve around lowering LDL levels, recent trials involving manipulations of the reverse cholesterol transport pathway by increasing HDL levels have shown promising results in the treatment of atherosclerosis: infusion of reconstituted HDL and synthetic ApoAI/phospholipid complexes has been shown in animals and humans to result in marked regression of atherosclerotic disease [Newton RS *et al*, 2002].

Apart from reverse cholesterol transport, HDL also protects against atherosclerosis via its roles in the inhibition of processes such as monocyte chemotaxis and LDL oxidation [Nofer JR *et al*, 2002; Bonnefont-Rousselot D *et al*, 1999], both of which are instrumental in the initiation of atherosclerotic plaque formation. At the heart of reverse cholesterol transport is the interaction between cells and lipoproteins, which results in cholesterol flux between the two. This flux consists of cholesterol efflux, cholesterol influx, and net cholesterol flux [Ji Y *et al*, 1997; Jian B *et al*, 1998]. The

discovery of proteins that mediate cholesterol movement between cells and acceptors such as the scavenger receptor, class B, type 1 (SR-BI) and ABCA1 have revitalized the study of the interaction between cells and lipoprotein, the flux of cholesterol, and its physiological implications [Rothblat GH *et al*, 2002].

1.2 Scavenger Receptor, Class B, Type I and Selective Uptake

The HDL receptor Scavenger Receptor, Class B, Type I (SR-BI) is a 509 amino acid integral membrane protein with a molecular weight of 84 kDa, which has been shown to have an important role in HDL-mediated reverse cholesterol transport [Krieger M, 2001]. It is composed of two transmembrane domains, a short N terminus, a slightly longer C terminus, and a large extracellular portion [Krieger M, 2001; Trigatti *et al*, 2000^a]. SR-BI is a member of the CD36 family of proteins, with 30% sequence homology to CD36, and is expressed in a variety of tissues [Trigatti BL *et al*, 2000^a]. SR-BI is abundant in liver hepatocytes and Kupffer cells in the liver, as well as steroidogenic tissues such as the adrenal glands, testes, and ovaries [Trigatti BL *et al*, 2000^a; Krieger M, 2001]. SR-BI is also present in macrophages, vascular endothelium, and a variety of other tissues [Krieger M, 2001]. It is a multi-ligand receptor that mediates binding of various ligands including HDL, LDL, modified HDL and LDL, apolipoproteins such as ApoA1 and ApoE, and modified (but not native) serum albumin [Trigatti BL *et al*, 2000^a; Krieger M, 2001; Acton S *et al*, 1996].

The process of cholesterol delivery to the liver and steroidogenic tissues via HDL was initially thought to be receptor independent [Krieger M, 2001]. It was later found to involve a unique process mediated by SR-BI called selective cholesterol uptake [Acton S *et al*, 1996; Trigatti BL *et al*, 2000^b]. In the case of the LDL receptor, bound lipoproteins are taken up via a well-characterized pathway involving endocytosis in clathrin-coated pits, with subsequent hydrolysis of LDL in lysosomes [Goldstein JL *et al*, 1985]. Like the LDL receptor, SR-BI mediates the uptake of cholesterol from lipoproteins via binding of the lipoprotein; however, cholesterol from HDL is taken up by SR-BI mediated selective uptake, where cholesteryl esters are transferred into cells from the hydrophobic core of the lipoprotein, without net internalization or subsequent degradation of the entire particle [Acton S *et al*, 1996]. After transfer of lipids, the lipoprotein particle is released back into the extracellular space [Trigatti BL *et al*, 2000^b; Krieger M, 2001]. The detailed mechanism behind the dissociation of lipids from proteins in selective uptake is not yet clear, but several mechanisms have been suggested. First, SR-BI may mediate this by providing a hydrophobic channel allowing lipid transfer by diffusion from the lipoprotein particle to the plasma membrane [Rodrigueza WV *et al*, 1999]. By hydrolyzing phospholipids on the surfaces of HDL and the plasma membrane, phospholipases such as hepatic lipase may help facilitate the transfer of lipid from lipoprotein to cell [Lambert G *et al*, 1999]. A second postulated mechanism involves transient internalization of the HDL particle into the early endosome system in the cell via SR-BI mediated endocytosis, with emptying of its cholesteryl ester components, and subsequent recycling and

transport of depleted HDL particles back to the membrane for resecretion [Silver DL *et al*, 2001]. The exact mechanism behind SR-BI mediated selective uptake is not yet clear.

As mentioned, CETP has been implicated in the facilitation of selective uptake. CETP facilitates the transfer of cholesteryl esters from HDL to apolipoprotein B (ApoB)-containing lipoproteins such as VLDL, IDL, and LDL [Yamashita S *et al*, 2001], and this remodeling by CETP is thought to further predispose HDL to selective uptake [von Eckardstein A *et al*, 2001]. Because mice do not express CETP, a much larger proportion of cholesteryl ester elimination in them is carried out via selective uptake, whereas selective uptake accounts for significantly less cholesteryl ester elimination in species that express CETP [Barter PJ *et al*, 2003]. Indeed, CETP is currently being studied as a therapeutic target in the treatment of atherosclerosis because CETP inhibitors have been shown to raise HDL concentration and decrease concentrations of LDL and ApoB [Barter PJ *et al*, 2003]. ApoE may also have a role in the mediation of selective uptake. In ApoE deficient mice, selective uptake is seen to be reduced [Arai T *et al*, 1999], suggesting that ApoE may also have a role in HDL-SR-BI interaction.

In cell culture studies, SR-BI has been shown to mediate cholesterol efflux from cells [Ji Y *et al*, 1997]. It has been seen that levels of cholesterol efflux from cells to HDL are related to the level of SR-BI expression in these cell types [Jian B *et al*, 1998]. The rate of cholesterol release shows most sensitivity at the lower concentrations of SR-BI; however, the rate is not proportional the level of SR-BI expression [Jian B *et al*, 1998; Rothblat G *et al*, 1999]. Further, cholesterol efflux to HDL is significantly increased from cells transiently transfected with SR-BI [Rigotti A *et al*, 1995]. Studies

conducted using stably transfected CHO or transiently transfected COS cells showed that SR-BI expression can stimulate bi-directional cholesterol flux by mediating efflux of cell cholesterol as well as influx of cholesterol from HDL [de la Llera-Moya M *et al*, 1999]. Some have suggested that SR-BI expression can stimulate cholesterol efflux to phospholipid vesicles not bound to SR-BI [Calvo D *et al*, 1998]. Studies with CD36 have demonstrated that although binding occurs with both SR-BI and CD36, lipid transport is only established with SR-BI [Gu X *et al*, 1998; de la Llera-Moya M *et al*, 1999]. In addition, experiments using an anti-mSR-BI blocking antibody have shown that blocking lipoprotein binding to SR-BI also blocked cholesterol efflux to HDL and LDL [Gu X *et al*, 2000]. Based on these data, binding seems to be important yet not sufficient for lipid transfer [Gu X *et al*, 1998; Gu X *et al*, 2000].

The fact that SR-BI is expressed most highly in the liver and steroidogenic tissues suggests that it is a physiologically relevant receptor. This is because these tissues have been shown to have the highest levels of selective HDL cholesteryl ester uptake [Krieger M, 2001]. Additionally, studies in transgenic and knockout mice, described next, have shown that SR-BI alteration has a corresponding effect on cholesterol metabolism.

1.3 Role of SR-BI in Various Physiological Systems

1.3.1 Role of SR-BI in Lipoprotein Metabolism

The role of SR-BI in lipoprotein metabolism and cardiovascular pathology has been revealed by studies conducted in mice lacking SR-BI, partially lacking SR-BI, and with hepatic overexpression of SR-BI on wild-type backgrounds as well as on various murine models of atherosclerosis. These models include: the ApoE knockout mouse, which is hypercholesterolemic and develops atherosclerosis spontaneously [Nakashima Y *et al*, 1994; Reddick RL *et al*, 1994], the LDL receptor knockout mouse, a murine model for familial hypercholesterolemia that develops diet-induced atherosclerosis [Breslow JL, 1996], and the human ApoB transgenic mouse model of diet-induced atherosclerosis [Purcell-Huynh DA *et al*, 1995; Callow MJ *et al*, 1995].

Wild-type mice normally have plasma cholesterol levels of ~100 mg/dl, primarily associated with a single lipoprotein, HDL [Rigotti *et al*, 1997]. ApoE knockout mice have plasma cholesterol levels of about 400 to 500 mg/dl [Breslow JL, 1996; Dansky HM *et al*, 1999], mainly due to collections of VLDL remnants and IDL/LDL sized lipoproteins [Plump AS *et al*, 1992]. Plasma cholesterol levels in LDL receptor knockout mice are not as elevated as in the ApoE knockout mouse, but are raised slightly to about 175 to 225 mg/dL [Ishibashi S, 1993], due to the appearance of LDL in the plasma. Human ApoB transgenic mice have plasma cholesterol levels of approximately 140 mg/dl on a chow diet [Purcell-Huynh DA *et al*, 1995].

When fed a high fat diet, both LDL receptor knockout and ApoE knockout mice develop severely elevated plasma cholesterol compared to mice on normal chow, from 2 to 5-fold, due to increased VLDL sized and IDL/LDL sized lipoproteins. [Plump AS *et al*, 1992; Breslow JL, 1996; Davis HR *et al*, 2001; Covey SD *et al*, 2003]. Human ApoB transgenic mice fed a high fat diet have total plasma cholesterol levels of about 310 mg/dl [Purcell-Huynh DA *et al*, 1995], due to increased synthesis and decreased clearance of human ApoB containing lipoproteins [Purcell-Huynh DA *et al*, 1995; Ueda Y *et al*, 2000].

Table 1 shows the effects of SR-BI manipulations in various backgrounds on lipoprotein metabolism and atherosclerosis. Adenovirus-mediated SR-BI overexpression in the liver results in decreased plasma cholesterol levels and increased biliary cholesterol [Kozarsky KF *et al*, 1997]. Although these mice show low levels of HDL in plasma, this is more indicative of increased clearance of cholesterol from plasma than the associated elevated risk for atherosclerosis. In transgenic mice with hepatic overexpression of SR-BI introduced by replacing the SR-BI promoter region with the human ApoAI promoter, HDL was seen to be decreased in plasma in both normal chow and fat fed mice [Ueda Y *et al*, 1999]. Similar results were seen in SR-BI transgenic mice created using the ApoE/C-I promoter [Wang N *et al*, 1998].

Conversely, SR-BI knockout mice show larger quantities of circulating HDL than wild-type mice in their lipoprotein profiles [Rigotti A *et al*, 1997]. In addition, these particles are abnormally large. This is believed to result from a lack of hepatic cholesterol clearance from the plasma [Rigotti A *et al*, 1997; Van Eck *et al*, 2003; Trigatti BL *et al*,

2000^a; Trigatti B *et al*, 2000^b, Mardones P *et al*, 2001]. In mice lacking SR-BI, biliary cholesterol is decreased, without any significant differences in bile acid or fecal bile secretion; bile acid pool size also remains unaltered [Mardones P *et al*, 2001]. These findings show that cholesterol uptake in the liver is reduced with SR-BI deletion, evidenced by lowered cholesterol secretion in bile, signifying the importance of SR-BI in the regulation of HDL metabolism, HDL cholesterol uptake and clearance (by steroidogenic tissues and/or the liver), and biliary cholesterol levels [Mardones P *et al*, 2001]. Supporting this are studies in SR-BI attenuated (SR-BIatt) mice. These mice have a mutation in the SR-BI promoter; in homozygous SR-BIatt mice, hepatic SR-BI expression is reduced by about 50%, total plasma cholesterol is increased by about 50-70% almost exclusively due to increased HDL, HDL particles are increased in size, and HDL phospholipids as well as ApoAI levels are raised [Varban M *et al*, 1998].

SR-BI is also known to mediate cholesterol clearance from ApoB containing lipoproteins such as VLDL and LDL. In fact, the initial identification of SR-BI as a scavenger receptor was based on its ability to bind acetylated LDL (AcLDL) [Acton S *et al*, 1994], and this binding property was the first used in defining scavenger receptors [Brown MS *et al*, 1983]. Studies involving SR-BI overexpression in the liver of wild-type mice have shown reduced levels of both ApoB and VLDL/LDL cholesterol in addition to HDL [Kozarsky KF *et al*, 1997; Ueda Y *et al*, 1999]. Moreover, in hemizygous human ApoB transgenic animals, mice fed normal chow showed reduced HDL and VLDL/LDL. However, when fed a high fat diet, only HDL was seen to be reduced, with normal VLDL and LDL levels [Arai T *et al*, 1999]. Interestingly, attenuated SR-BI levels in LDL

receptor knockout mice showed increased ApoB and LDL levels compared to LDL receptor knockout mice with normal levels of SR-BI; this was found to be due to increased LDL cholesterol production rather than reduced clearance, suggesting that increased atherosclerosis due to down-regulation of SR-BI may result partially from increased LDL cholesterol [Huszar D *et al*, 2000]. Complete deletion of SR-BI in mice on an ApoE *-/-* or LDL receptor *-/-* backgrounds, however, showed raised total cholesterol due to large HDL particles, and reduced ApoB and LDL cholesterol [Trigatti B *et al*, 1999; Covey SD *et al*, 2003]. The reduced ApoB and LDL may be a result of altered VLDL/LDL secretion resulting from altered HDL uptake [Sniderman *et al*, 2003].

These findings point to a strong role for SR-BI in cholesterol and lipoprotein metabolism and clearance, and suggest a significant role for SR-BI in the pathogenesis of atherosclerosis.

1.3.2 Role of SR-BI in Cardiovascular Pathology

Lack of SR-BI has been shown to markedly accelerate atherosclerotic development in both ApoE and LDL receptor knockout mice [Trigatti B *et al*, 1999 ; Braun A *et al*, 2002; Covey SD *et al*, 2003]. SR-BI/ApoE double knockout mice fed normal chow show marked atherosclerosis development within a few weeks of age and die at an average of about 6 weeks of age from extensive coronary occlusions and myocardial infarctions [Braun A *et al*, 2002] in contrast to ApoE single knockout mice, which normally live over 1 year and develop less severe atherosclerosis [Calara F *et al*, 2001]. These findings have suggested that SR-BI is protective against atherosclerosis.

A summary of the effects of SR-BI manipulations on atherosclerosis in mice with various genetic backgrounds is shown in Table 1. Atherosclerosis is generally seen to be reduced with SR-BI overexpression, presumably due to increased clearance of HDL and non-HDL cholesterol [Kozarsky KF *et al*, 2000; Arai T *et al*, 1999]. The exception is seen in human ApoB-transgenic mice fed a high fat diet, in which 2-fold hepatic SR-BI overexpression resulted in decreased atherosclerosis, whereas 10-fold overexpression resulted in three times more atherosclerosis than with 2-fold overexpression, indicating that extremely high levels of SR-BI expression may result in a pro-atherogenic state that could potentially be a result of marked changes in lipoprotein structure, composition, and function [Ueda Y *et al*, 2000]. Atherosclerosis is seen to increase in wild-type or LDL receptor knockout mice lacking SR-BI placed on a high fat diet [Covey SD *et al*, 2003, Van Eck *et al*, 2003]. However, as described, SR-BI/ApoE double knockout mice show dramatically accelerated atherosclerosis development on a normal chow diet, associated with premature mortality [Braun A *et al*, 2002].

The antioxidant drug probucol can be used to help overcome the effects seen in the SR-BI/ApoE double knockout mouse [Braun A *et al*, 2003]. ProbucoL has been shown to rescue infertility in SR-BI *-/-* females [Miettinen H *et al*, 2001, Introduction, *1.3.3 Role of SR-BI in the Female Reproductive System*]. It also has recently been seen that probucol can rescue the premature mortality seen in SR-BI/ApoE double knockout mice, extending lifespan from 6 weeks to up to 60 weeks. It has been shown to almost completely reverse all cardiac and most erythrocyte abnormalities, as well as abnormal lipoprotein

morphologies seen in SR-BI/ApoE double knockout mice, by about 5-6 weeks of age [Braun A *et al*, 2003].

1.3.3 Role of SR-BI in the Female Reproductive System

SR-BI knockout female mice are infertile, and their ovaries have been seen to have significantly reduced lipid stores, again consistent with the idea that SR-BI mediates selective uptake of cholesterol into cells; however, their estrus cycles and ovulation patterns are not significantly different from their wild-type counterparts [Trigatti B *et al*, 1999; Krieger M, 2001]. Other murine homozygous knockout mutants [LCAT, acyl-coA cholesterol acyl transferase (ACAT), and ApoAI] show similar lipid-depletion patterns in steroidogenic tissues without infertility; also, relatively normal levels of estrogen and progesterone in SR-BI knockout mice indicate that steroid hormone biosynthesis activity is adequate in these models [Trigatti B *et al*, 1999]. On further analysis, viability studies have shown that alterations in morphology of oocytes from SR-BI knockout females seem to have a role in the arrested development of embryos in these mice [Krieger M, 2001; Trigatti B *et al*, 1999].

SR-BI knockout females have been shown to regain fertility with administration of the drug probucol [C₃₁H₄₈O₂S₂: 516.84; 4, 4' - Isopropylidenedithio - bis (2,6 - di - tert - butyl - phenol)], a cholesterol-lowering, anti-atherogenic antioxidant drug [Miettinen H *et al*, 2001]. Inactivation of the ApoA1 gene can also rescue infertility in SR-BI knockout females [Miettinen H *et al*, 2001]. In light of these findings, it is likely

that infertility in SR-BI knockout females is the result of abnormal lipoprotein metabolism. As mentioned, other female homozygous mutants with low plasma cholesterol levels retain fertility; therefore, it seems that low plasma cholesterol is not the primary phenomenon leading to loss of fertility in female SR-BI knockout mice. It has been suggested that specific abnormalities in the composition and structure of lipoproteins may be responsible for this phenotype [Miettinen H *et al*, 2001; Krieger M, 2001]. For instance, HDL normally contains the lipid soluble Vitamin E [Mardones P *et al*, 2002]. Vitamin E is transported in lipoproteins and is required for murine female fertility; it may be delivered to cells via SR-BI [Mardones P *et al*, 2002], along with other fertility factors, and hindrances in delivery may result in disruptions in important ovarian functions and normal oocyte production [Miettinen H *et al*, 2001]. Although there is a lot yet to uncover, this information suggests that the primary reason for infertility in SR-BI knockout females has more to do with abnormal lipoprotein structure and metabolism than with alterations in plasma cholesterol levels or with a direct effect of a lack of SR-BI in the ovary.

1.3.4 Role of SR-BI in the Gastrointestinal System

In the gastrointestinal system, SR-BI is expressed on the apical surfaces of intestinal epithelial cells, and *in vitro* cell culture studies have shown that SR-BI may have a role in cholesterol absorption [Hauser H *et al*, 1998]. As mentioned, SR-BI knockouts and SR-BI^{att} mice both show a decrease in biliary cholesterol levels, in the

absence of altered absorption or fecal sterol excretion in mice lacking functioning SR-BI [Trigatti B *et al*, 1999; Ji Y *et al*, 1999; Mardones P *et al*, 2001]. This indicates that although SR-BI may have a role in intestinal absorption of cholesterol, there are likely several effective compensatory mechanisms at play that result in normal cholesterol absorption rates in SR-BI knockout mice [Krieger M, 2001; Mardones P *et al*, 2001]. Whereas hepatic expression of SR-BI plays a critical role in HDL-associated cholesterol metabolism, intestinal expression of SR-BI does not seem to be essential for adequate cholesterol absorption [Mardones, P *et al*, 2001].

1.3.5 Effects of SR-BI on Erythrocyte Morphology

SR-BI has also been shown to have an effect on erythrocyte morphology. SR-BI knockout mice show disruptions in late erythroid differentiation [Holm TM *et al*, 2002]. These morphological abnormalities are more pronounced with marked hypercholesterolemia, as seen in the SR-BI/ApoE double knockout mouse; in contrast to ApoE single knockout mice showing normal erythrocyte morphology, erythrocytes from SR-BI double knockout mice show characteristics of intermediates in reticulocyte differentiation such as macrocytosis, irregular shape, and large autophagosomes [Krieger M, 2001; Holm TM *et al*, 2002; Covey SD *et al*, 2003].

These effects are likely due to increased cholesterol content in cells; expulsion of autophagosomes can be induced *in vitro* by cholesterol removing agents such as methyl β cyclodextrin, or *in vivo* by infusing abnormal cells into SR-BI expressing mice [Holm

TM *et al*, 2002]. Furthermore, abnormal erythrocyte morphology can be corrected with probucol [Braun A *et al*, 2003]. This suggests that this phenotype results from altered lipoprotein metabolism and/or lipoprotein structure in these cells [Holm TM *et al*, 2002; Braun A *et al*, 2003; Covey SD *et al*, 2003].

Manipulation		Genetic background	HDL Cholesterol	VLDL/LDL Cholesterol	Atherosclerosis
Liver Overexpression	Adenovirus-mediated [1,2]	Wild type	Decreased [1]	Decreased [1]	Decreased [2]
		LDL receptor KO ¹	Decreased [2]	No effect [2]	
	Transgenic [ApoA-I promoter] [3,4]	Wild type Human apoB transgenic	Decreased [3] Decreased [4]	Decreased [3] Minimal difference [4]	Decreased in mice with 2x-overexpression [4] No reduction in mice with 10x overexpression [4]
	Transgenic [ApoE promoter] [5,6]	Wild type Heterozygous LDL receptor mutant	Decreased [5] Decreased [6]	Decreased [5] Increased [6]	Decreased [6]
Reduction of SR-BI	SR-BI KO	Wild type [7,15]	Increased cholesterol associated with large size HDL [7,8,15,16]	No change on chow Decreased on HF ² diet [8]	Increased diet induced [15]
		ApoE KO [16] LDL receptor KO [8]			Increased on chow [16] Increased diet induced [8]
	SR-BI att	Wild type	Increased [11]	No effect [11]	Increased on HF diet [13]
		ApoE KO	No effect [14]	No effect [14]	
		LDL receptor KO	No effect [13]	Increased on HF diet [13]	

Table 1. Effects of SR-BI manipulation on plasma lipoprotein cholesterol levels and atherosclerosis in mice with various genetic manipulations. [References for Table 1 on the following page].

¹ KO: knockout

² HF: high fat

References for Table 1:

1. Kozarsky KF *et al*, 1997
2. Kozarsky KF *et al*, 2000
3. Ueda Y *et al*, 1999
4. Ueda Y *et al*, 2000
5. Wang N *et al*, 1998
6. Arai T *et al*, 1999
7. Rigotti A *et al*, 1997
8. Covey SD *et al*, 2003
9. Braun A *et al*, 2002
10. Sehayek E *et al*, 1998
11. Varban ML *et al*, 1998
12. Ji Y *et al*, 1999
13. Huszar D *et al*, 2000
14. Arai T *et al*, 1999
15. Van Eck M *et al*, 2003
16. Trigatti B *et al*, 1999

1.4 Macrophage SR-BI and Bone Marrow Transplantation

SR-BI is expressed in macrophages [Krieger M, 2001] and macrophages are directly involved in atherosclerotic plaque development [Schwartz CJ *et al*, 1991; de Villiers WJ *et al*, 1999]. As mentioned, deletion of SR-BI accelerates atherosclerosis development in both ApoE and LDL receptor knockout mice. A major component in the anti-atherogenic effects of SR-BI has to do with increased hepatic clearance of cholesterol from plasma [Mardones P *et al*, 2001] as described. It is also known that SR-BI mediates cholesterol efflux from cells to lipoprotein acceptors [Ji Y *et al*, 1997]. What is the physiological relevance of SR-BI in macrophages *in vivo*? Potentially, does SR-BI in macrophages have a contributing role in cardiovascular pathology? Whether SR-BI can facilitate efflux of cholesterol from macrophages to HDL *in vivo* has not yet been established. Based on its properties in mediating bi-directional flux, SR-BI in macrophages may play an important anti-atherogenic role presumably by facilitating efflux to HDL or, alternatively, mediate cholesterol delivery to macrophages and thus accelerate foam cell formation.

An effective and efficient method to study the roles of genes in macrophages is via bone marrow transplantation and the creation of chimeric mice. Macrophages are derived from monocytes, which originate in the bone marrow; therefore, bone marrow transplantation makes available a method whereby selective genetic alterations can be introduced into bone marrow derived cells, including macrophages [Linton MF, 1999; Herjgers N *et al*, 1997]. This technique has been used, for example, to test the role of

ApoE in mouse macrophages, where ApoE $-/-$ bone marrow cells were transplanted into wild-type mice, showing an increase in atherosclerosis compared to control wild-type mice transplanted with ApoE $+/+$ bone marrow [Fazio S *et al*, 1997]. Bone marrow transplantation has also been used to create chimeric mice (on an LDL receptor knockout background) expressing ApoE only in bone marrow derived cells, showing that physiological expression of ApoE in macrophages reduced atherosclerosis in hyperlipidemic mice [Fazio S *et al*, 2002]. Similar studies have been carried out to test the role of proteins implicated in cholesterol efflux such as ABCA1 [Aiello R *et al*, 2002]. ABCA1 encodes a membrane protein that facilitates cholesterol efflux from cells to lipid-deficient ApoAI; homozygous mutations in ABCA1 result in Tangier disease, characterized by accumulation of cholesterol-laden macrophages and HDL deficiency [Rust S *et al*, 1999]. R. Aiello and colleagues used bone marrow transplantation to create chimeras with ABCA1 selectively knocked out in bone marrow derived cells, showing that atherosclerosis increased in ApoE knockout as well as LDL receptor knockout mice that lacked functioning ABCA1 in macrophages [Aiello R *et al*, 2002; van Eck M *et al*, 2002]. The role of macrophage fatty-acid-binding protein aP2 (a protein involved in the regulation of systemic insulin resistance and lipid metabolism) in atherosclerosis has also been tested via bone marrow transplantation, showing increased atherosclerosis in mice with aP2 null macrophages [Makowski L *et al*, 2001; Layne MD *et al*, 2001].

Bone marrow transplantation has thus been used widely as a method to test the roles of specific proteins in macrophages and their contribution to the development of or protection against atherosclerosis.

Using bone marrow transplantation to create chimeric mice selectively lacking functional SR-BI in bone marrow derived cells has shed light on the physiological relevance of macrophage SR-BI on atherogenesis. This may open up new avenues of research into the mechanisms by which macrophage SR-BI confers these effects *in vivo*. Atherosclerosis development in hyperlipidemic chimeric mice (of an ApoE or LDL receptor knockout background) lacking normal, functioning SR-BI in bone marrow derived cells was compared to mice possessing normal, functioning SR-BI in bone marrow derived cells as a test to see what role macrophage SR-BI plays in the development of atherosclerosis. This can also indicate whether macrophage SR-BI is a contributing factor in the overall anti-atherogenicity conferred by SR-BI in mice.

Recently, Scott Covey, a colleague in the laboratory found that selective elimination of SR-BI expression in bone marrow derived cells increased diet-induced atherosclerosis development in LDL receptor knockout mice [Covey SD *et al*, 2003]. My project has centered on looking at the effects of bone marrow-specific SR-BI deletion on atherosclerosis development in ApoE knockout mice.

1.5 Project Overview

To study the role of SR-BI in macrophages in hyperlipidemic mice (ApoE $-/-$), bone marrow transplantation was used to generate chimeric mice lacking SR-BI in bone marrow derived cells, including monocytes and macrophages. Bone marrow cells from mice either lacking or possessing normal levels of SR-BI were transplanted into recipient mice and the development of atherosclerosis in these chimeric mice was determined.

I used inbred female C57Bl/6 ApoE knockout mice as recipients to reduce variability due to genetic background differences, and due to their elevated susceptibility to developing atherosclerosis compared to mice of mixed or other genetic backgrounds [Fazio S *et al*, 2001; Dansky HM *et al*, 1999]. Mixed background SR-BI $+/+$ ApoE $-/-$ control or SR-BI $-/-$ ApoE $-/-$ mice were used as donors. The effect of altering SR-BI in macrophages on atherosclerotic development was assessed histologically via analysis of aortic root cross sections and measurement of plaque surface area in mouse aortas. The effect of elimination of macrophage SR-BI on plasma cholesterol levels and lipoprotein profiles was also assessed via analysis of blood samples from these mice.

The project was geared towards the following objectives:

1. To establish conditions for bone marrow repopulation of C57BL/6 ApoE knockout mice.
2. To use bone marrow transplantation to generate ApoE knockout mice selectively SR-BI-deficient in bone marrow derived cells.

3. To determine the effect of selective SR-BI deficiency in bone marrow derived cells of ApoE knockout mice on lipoprotein cholesterol levels.
4. To determine the effect of selective SR-BI-deficiency in bone marrow derived cells of ApoE knockout mice on diet induced atherosclerosis in the aortic sinus and proximal and distal aorta.

1.6 Hypothesis

We predict that SR-BI in macrophages contributes to the athero-protective effect of SR-BI as demonstrated in transgenic and knockout animals. Whereas hepatic SR-BI contributes to this effect via cholesterol uptake, macrophage SR-BI may do so via mediating cholesterol efflux from cells to HDL, as it has been shown to do *in vitro*.

2. Materials and Methods

2.1 Materials

Chemicals and reagents used are listed in Table 2.

Table 2. Reagents and Suppliers

Chemical/Reagent	Supplier
Acetone	BDH
Agarose	GibcoBRL
Ammonium Chloride	BDH
Ammonium Sulfate	BDH
Anti-CD11b (MAC-1)-biotinylated antibody	PharMingen, Catalog # 01712D
Aquaperm Mounting Medium	ThermoShandon
β -mercaptoethanol	Sigma
Bovine Serum Albumin	GibcoBRL
Cholesterol Stock Solution 2 g/l	Wako Chemicals
Cryomatrix	ThermoShandon
dATP, dCTP, dGTP, dTTP (all 100 mM)	MBI Fermentas
Dimethyl Sulfoxide (DMSO)	Sigma
EDTA	BDH
Ethidium Bromide	Sigma
Fc Blocker/Purified CD16/CD32	PharMingen, Catalog # 553141
Fetal Bovine Serum	GibcoBRL, Sigma
10% Formaldehyde Solution	Sigma
37% Formaldehyde Solution	ACP
L-Glutamine	Invitrogen
Glycerol-Gelatin	Sigma
Heparin	Sigma
High Fat Western-Type Mouse Diet	Harlan Teklad, Dyets
Hydrogen Chloride	EM Science
Infinity Cholesterol Liquid Stable Reagent Kit	ThermoDMA
Iscove's Medium	GibcoBRL
Isoflurane	Abbott Laboratories
Isopropanol	Sigma, ACP
Jell-O	Kraft

Lactated Ringer's Injection USP	Baxter Corporation
Magnesium Chloride	EM Science
Mayer's Hematoxylin	Sigma
2-Methyl-2-Butanol	Fischer
2-Methylbutane	EM Science
Normal Chow Mouse Diet	Harlan Teklad (#7004; #7904 irradiated)
NucleoSpin Blood Quick Pure Mini Kit	BD Biosciences, Clontech
NutriCal (Nutritional Supplement Paste)	Tomlyn Products
Oil Red O	Sigma
Penicillin-Streptomycin	GibcoBRL
Potassium Chloride	Bioshop
Potassium Dihydrogen Orthophosphate	BDH
Probuco Mouse Diet (0.5% Probuco)	TestDiets
Proteinase K	Roche
SDS	Bioshop
Sodium Azide	J.T. Baker Chemical Co.
Sodium Chloride	Bioshop
Sodium Dihydrogen Orthophosphate	Bioshop
SR-BI Primer, oDT44, common	Mobix
SR-BI Primer, oDT66, wild-type specific	Mobix
SR-BI Primer, Si75, neo-specific	Mobix
Streptavidin-Cy-Chrome (Cy5) Conjugate	PharMingen, Catalog # 554062
Sudan IV	Sigma
Taq Polymerase	Promega
2,2,2 Tribromoethanol	Aldrich
Trimethaprim-Sulfamethoxazole (Apo Sulfa-Trim)	Apotex Inc.
Tris	Bioshop

2.2 Methods

2.2.1 Generation and Maintenance of Mice

C57Bl/6 ApoE $-/-$ or C57Bl/6 LDLR $-/-$ founders (backcrossed 10 times) were obtained from Jackson Laboratories (<http://www.jax.org>) and bred in the Barrier Unit of the Central Animal Facility at the McMaster University Health Sciences Centre. SR-BI $+/-$ ApoE $-/-$ mice on a mixed C57Bl/6 x 129 Agouti genetic background were obtained from Dr. Monty Krieger at the Massachusetts Institute of Technology, and mated to generate SR-BI $+/+$ ApoE $-/-$ and SR-BI $-/-$ ApoE $-/-$ donor mice. Green fluorescent protein (GFP) transgenic mice were provided by Dr. Masaru Okabe at the Osaka University, Japan. After irradiation and/or transplantation, mice were housed in an ultra-clean “biobubble” facility in the main Central Animal Facility at the McMaster University Health Sciences Centre.

Female C57Bl/6 ApoE $-/-$ mice were used as bone marrow recipients. Recipients received bone marrow cells from male SR-BI $+/+$ ApoE $-/-$ (control group) or SR-BI $-/-$ ApoE $-/-$ (experimental group) donor mice on a mixed genetic background.

Due to the infertility of SR-BI $-/-$ female mice [Trigatti B *et al*, 1999], limitations on the generation of SR-BI $-/-$ ApoE $-/-$ donor mice necessitated regular genotyping of mice generated from breeding pairs in which females were heterozygous for SR-BI and the males were either heterozygous or homozygous for mutant SR-BI. This problem was

handled successfully later on during the course of the project, when we obtained the drug probucol to rescue the infertility of the female SR-BI $-/-$ breeders.

Recipient mice were maintained on a normal chow diet. Donor mice and the breeders used to generate them were maintained on a diet containing the drug probucol (0.5% probucol) [Miettinen H *et al*, 2001] to aid the generation of desired offspring (see *1.3 Role of SR-BI in Various Physiological Systems*). Probucol can also be administered to breeding pairs with homozygous SR-BI knockout females, allowing for efficient and expedient generation of SR-BI knockout mice [Miettinen H *et al*, 2001].

Breeding pairs and pups were housed in separate rooms. Pups were separated from parents at 3 weeks of age, and males and females housed in separate cages.

2.2.2. Preparation of DNA from Mouse Tail Biopsies

Two days after weaning, mice were anesthetized using the inhalational anesthetic Isoflurane. Numbered identification was assigned to mice via ear tags. Tail samples were obtained for genotyping by cutting approximately 1 cm of tail with a clean razor blade. Bleeding ends were cauterized, and samples were placed in 400 μ l tail lysis buffer (200 mM NaCl, 40 mM Tris pH 8.0, 20 mM EDTA, 0.5% SDS, and 0.5% β -mercaptoethanol) with 20 mg/ml Proteinase K in a 1.5 ml microtube [Laird PW *et al*, 1991]. Tail samples were digested overnight at 55°C, vortexed periodically during digestion, and centrifuged at 14,000 rpm for 10 minutes. Supernatant containing DNA was transferred to a fresh tube, 1 ml of 99% isopropanol was added, and precipitation of DNA was brought about

by inverting the tube several times [Laird PW *et al*, 1991]. The whitish strands of precipitated DNA were lifted out using a clean pipette tip and transferred to a fresh tube. After approximately 30 minutes to 1 hour of drying time, DNA was placed in 0.2 ml TE (pH 8.0) buffer overnight at 37°C for complete dissolution [Laird PW *et al*, 1991]. 4 µl DNA solution was diluted 100-fold in ddH₂O.

PCR was used to identify wild type and mutant alleles for each mouse. (*see 2.2.8. PCR Genotyping*).

2.2.3. Collection of Blood

Mice were anesthetized using the injectable anesthetic Avertin (2.5 g 2,2,2-tribromoethanol, 5 ml 2-methyl-2-butanol, diluted to a 2.5% concentration in PBS, neutral pH). 0.3-0.5 ml 2.5% Avertin in PBS was injected intraperitoneally for anesthesia in mice to collect blood for flow cytometric analysis, PCR genotyping, or plasma analysis for cholesterol and lipoprotein levels prior to being placed on a high fat diet. Once anesthetized, mice were bled through the tail vein, by cutting approximately 1 cm of the tail end and the tail was “milked” with the fingers, allowing blood to collect in a 1.5 ml microtube containing 1 µl of the anticoagulant heparin (10,000 U/ml PBS). The tube was inverted and gently shaken sporadically to allow heparin to mix with the blood. An average of ~150 µl blood per mouse was collected by this method.

For exsanguination by cardiac puncture, a lethal dose of approximately 0.8-0.9 ml 2.5% Avertin in PBS was injected intraperitoneally. A 1 ml syringe was heparinized by

loading approximately 10-20 μ l heparin (10,000 U/ml PBS) to coat the walls of the syringe. A 25G $\frac{5}{8}$ needle was used to collect blood in the syringe by cardiac puncture, carried out by insertion of the needle just under the left subcostal margin, close to the sternum, and further into the left ventricle of the heart, from which blood was gently drawn. Collected blood was transferred to a fresh heparinized 1.5 ml microtube (1 μ l heparin, 10,000 U/ml PBS), and mixed. An average of \sim 0.8 ml blood per mouse was collected by this method.

2.2.4. Preparation of Plasma and Analysis of Plasma and Lipoprotein Cholesterol

For plasma analysis, blood was collected by tail vein bleeding at 4 weeks post-transplantation (before placing mice on a high fat diet). For analysis at the end of the 12 week period during which mice were fed a high fat diet, blood was collected by cardiac puncture (see 2.2.3. *Collection of Blood*). Blood samples were centrifuged at 14,000 rpm for 5 minutes at 4°C, and plasma (supernatant) containing lipoproteins was isolated and transferred to a fresh tube. Plasma samples from mice in the same group (experimental or control) were pooled, and lipoproteins were separated by size from 0.1 ml pooled plasma by gel filtration chromatography using an AKTA FPLC with a Superose 6 HR 10/30 column and 154 mM NaCl/1 mM EDTA, pH 8 (lipoprotein FPLC buffer) as the elution solution [Rigotti A *et al*, 1997]. 0.25 ml fractions were assayed for total cholesterol levels using a coupled enzymatic assay comprised of cholesterol esterase, cholesterol oxidase, and peroxidase (Infinity Cholesterol Liquid Stable Reagent Kit) [Allain CC *et al*, 1974; Roeschlau P *et al*, 1974] with the reactions shown in Table 3.

Table 3. Coupled enzymatic assay (Infinity Cholesterol Liquid Stable Reagent Kit) kinetics.

Substrate/Reactants	Enzyme	Products
Cholesterol Esters	Cholesterol Esterase	Cholesterol + Fatty Acids
Cholesterol + O ₂	Cholesterol Oxidase	Cholest-4-en-3-one + H ₂ O ₂
2H ₂ O ₂ + hydroxybenzoic acid + 4-aminoantipyrine	Peroxidase	Quinoneimine Dye + 4H ₂ O

Each 0.25 ml fraction was mixed and 0.05 ml was diluted 2-fold with lipoprotein FPLC buffer to a total volume of 0.1 ml on a 96 well plate. 0.2 ml reagent was added to each sample. The samples were incubated at 37°C for 30 minutes and absorbance values at 500 nm were determined using a 96 well plate reader machine. Standard curves were plotted based on a range covering 0-30 µg cholesterol, from a cholesterol stock solution (2 g/l). The quantity of total cholesterol in each sample was determined based on the linear equation, and corrected to total cholesterol in mg/dl of plasma per fraction. These data were used to generate lipoprotein profiles. Total cholesterol levels (mg/dl of plasma) for each fraction were plotted against fraction number for both the experimental and control groups, before and after administration of the high fat diet.

Original plasma samples were also assayed for total plasma cholesterol levels. In this case, 1 µl of sample was diluted 100-fold with the described lipoprotein FPLC

buffer, and the assay technique described was applied using the same range of cholesterol amounts for standard curves.

2.2.5. Bone Marrow Transplantation

Male donor mice with genotypes SR-BI^{+/+} ApoE^{-/-} or SR-BI^{-/-} ApoE^{-/-} were euthanized by carbon dioxide asphyxiation and cervical dislocation. In the case of experiments to test for repopulation by flow cytometry (*Results, 3.1 Conditions for Bone Marrow Transplantation and Repopulation*), donor mice were ApoE^{-/-} and green fluorescent protein (GFP) transgenic. Donor mice were then sprayed with ethanol, a superficial incision was made in the abdomen, and abdominal skin was removed, keeping the peritoneal membrane intact. Femurs and tibias were removed and dissected free of extraneous tissue using autoclaved instruments. Bones were placed in a 35 mm cell culture dish containing Iscove's medium with 2% heat-inactivated fetal bovine serum supplemented with 2 mM L-glutamine and 50 mg/ml-50 U/ml penicillin-streptomycin. Under sterile conditions in the tissue culture hood, the ends of bones were cut with sterile instruments, and bone marrow was flushed out of the bones with Iscove's medium (with supplementations described previously) using a 26G½ needle and 1 ml syringe, from both ends of each bone. Cells were placed in the same media and cell culture dishes were kept on ice. Bone marrow cells were dispersed by passage through a 21 G needle twice and through a 26 G needle 4 times. Cells were filtered using a 100 µm cell strainer (Falcon)

into a sterile 5 ml tube and kept on ice. The total volume of each suspension was adjusted to 400-500 μ l with media with the goal to transplant a volume of 200 μ l ($\sim 7.5 \times 10^6$ cells) into each mouse.

Female C57Bl/6 ApoE^{-/-} recipient mice were irradiated during two sessions three hours apart to ablate their bone marrow. A total dose of 1000 cGy or 900 cGy was divided into 600 cGy and either 400 cGy or 300 cGy. Irradiation was carried out using either a cobalt (Co-60) source in the hot cell at the McMaster Nuclear Reactor facility, or a cesium (Cs-137) γ source in the ultra-clean “biobubble” facility mentioned above.

After irradiation, recipients were anesthetized via the administration of intraperitoneal injections of 0.3-0.4 ml 2.5% Avertin in PBS. Mice were placed on their sides on a cushion of autoclaved paper towels, and eyelids retracted until the eye bulged out. A 1 ml syringe containing 200 μ l of bone marrow cell suspension was used to inject cells intravenously into the retro-orbital plexus of the recipient mouse through a 26G $\frac{1}{2}$ needle perpendicularly inserted 2-3 mm deep through the conjunctiva into the eye socket behind the eyeball. Bone marrow cells harvested from a single donor were injected into the retro-orbital venous plexuses of two recipients ($\sim 7.5 \times 10^6$ cells per mouse).

Using SR-BI/ApoE double knockout mice as donors had the limitation that these mice die at ~ 6 -8 weeks of age [Braun A *et al*, 2002]; for this reason, careful coordination was required to ensure that recipient mice reached the age of 12 weeks, the age at which they are transplanted, at a time when SR-BI/ApoE double knockout mice were within their range of life. To counter this, donor mice in both experimental and control groups were fed a diet containing probucol, a drug useful in this case for its lipid-lowering, anti-

atherogenic, and antioxidant properties [Braun A *et al*, 2003], and shown to rescue early mortality in SR-BI/ApoE double knockout mice as well as infertility in SR-BI knockout females as mentioned [Miettinen H *et al*, 2001; Braun A *et al*, 2003]. Probucol was administered to both SR-BI^{+/+} ApoE^{-/-} and SR-BI^{-/-} ApoE^{-/-} donor mice awaiting bone marrow harvesting, making up 0.5% of the composition of their diets. This extended their lifespan and allowed for better coordination of donor-recipient co-availability for experiments.

For about 4 to 7 days before transplantation, mice in both groups were also given water containing 6.25 ml 40 mg/ml trimethaprim and 8 mg/ml sulfamethoxazole per 200ml (1.25 mg/ml trimethaprim, 0.25 mg/ml sulfamethoxazole, final concentrations), to help accustom them to antibiotic-containing drinking water and also to prophylactically counter infection during the immediate post-radiation stage. After transplantation, all mice were daily given water containing trimethaprim-sulfamethoxazole at the concentrations described above, Jell-O containing the same concentration of trimethaprim-sulfamethoxazole, powdered food with nutritional supplement paste (NutriCal) dissolved in water, and dry pelleted food for a period of two weeks.

2.2.6. Induction of Atherosclerosis

Four and a half weeks after transplantation, mice were fasted for 14-16 hours, and blood samples were obtained from mice by tail vein bleeding for the purpose of assessing bone marrow reconstitution by PCR and analysis of plasma for cholesterol levels (see

2.2.3. *Collection of Blood*). The mice were then placed on a high fat western-type diet (Harlan Teklad, Dyets: 42% fat, 0.15% cholesterol) to accelerate the development of atherosclerosis. After twelve weeks on the high fat diet, mice were again fasted for 14-16 hours, euthanized via a lethal intraperitoneal dose of 2.5% Avertin in PBS, and blood was collected (see 2.2.3 *Collection of Blood*) for assessment of plasma cholesterol and lipoprotein levels. Aortas and hearts were harvested for histological analysis.

2.2.7. Preparation of Blood Cell DNA

Four and a half weeks after transplantation, mice were anesthetized using Avertin and blood was withdrawn from their tail veins into 1.5 ml heparinized microtubes (see 2.2.3. *Collection of Blood*). 50 μ l of collected blood was used for DNA isolation and bone marrow reconstitution assessment by PCR. DNA from blood samples was isolated using a NucleoSpin Blood Quick Pure Mini kit. 5 μ l of the eluted DNA (total volume 50 μ l) was diluted 5-fold with ddH₂O, and samples were genotyped using PCR for wild-type and mutant SR-BI alleles. (see 2.2.9. *PCR Genotyping*).

2.2.8. Flow Cytometric Analysis of Blood Cells

Four and a half weeks after transplantation with GFP-transgenic bone marrow in the same way as described in 2.2.5 *Bone Marrow Transplantation*, blood was withdrawn from mice by tail bleeding for flow cytometric analysis (see 2.2.3. *Collection of Blood*).

30 μ l of each blood sample was placed in individual wells on a round-bottomed 96 well tray. 0.1 ml of Tris-NH₄Cl (17 mM Tris, 0.747% NH₄Cl, filter sterilized) was added to the blood samples, and samples were incubated at 37°C for 10 minutes for lysis of red blood cells. Samples were centrifuged at 4°C at 1000 x g for 3 minutes, and supernatants were removed. Again, 0.1 ml Tris-NH₄Cl was added and incubation and centrifugation was repeated as above. Supernatants were removed, and pellets were washed with ice cold FACS (fluorescence activated cell sorting) buffer (PBS with 0.1% BSA and 0.1% sodium azide), centrifuged again as above, and supernatants removed.

Apart from those cells representing the non-CD11b controls, cells were labelled first with Anti-CD11b (MAC-1)-biotinylated antibody (0.5 mg/ml). For each sample, originally from 30 μ l blood, cells were suspended in 50 μ l labeling solution (50 μ l FACS buffer, 0.5 μ l antibody, 0.1 μ l Fc blocker¹ or purified CD16/CD32, 0.5 mg/ml) and incubated at 4°C for 30 minutes in the dark. Cells were then centrifuged at 4°C at 1000 x g for 3 minutes. Supernatants were drained and cells were washed with ice cold FACS buffer as above. Following this, secondary labeling solution was added containing Streptavidin-Cy-Chrome (Cy5) conjugate² (0.2 mg/ml). In this case, 0.3 μ l Streptavidin-Cy-Chrome conjugate was added to 50 μ l ice cold FACS buffer, but with no Fc block.

¹ Antibody that reacts specifically with a common nonpolymorphic epitope on extracellular domains of mouse Fc γ III and Fc γ II receptors (Unkeless JC, 1979; Ravetch, JV *et al*, 1986), as well as possibly the Fc γ I receptor (Unkeless JC, 1979), therefore blocking non-antigen-specific binding of immunoglobulins to the Fc γ III, Fc γ II, and potentially the Fc γ I receptor.

² Absorption maximum 650 nm, emission maximum 670 nm, (<http://www.bdbiosciences.com/pharmingen/protocols/Fluorochrome>).

Again, the suspended cells were incubated in secondary labeling solution for 30 minutes at 4°C in the dark.

Cell suspensions were centrifuged as above and supernatants were drained. Cells were then washed twice with ice-cold FACS buffer and resuspended in 0.1 ml of the same. They were then filtered through a 50 µm nylon mesh (Sefar) and transferred to small 5 ml clear, round-bottomed, snap cap tubes (Falcon, Catalog # 352058). Flow cytometric analysis of cells was carried out on a FACSVantage at the Flow Cytometry Facility at the McMaster Health Sciences Center by Hong Liang.

2.2.9. PCR Genotyping

20 µl of a PCR master mix was added to 5 µl of diluted DNA prepared either from tail biopsies (see 2.2.2. *Preparation of DNA from Mouse Tail Biopsies*) or blood cell DNA (see 2.2.7. *Preparation of Blood Cell DNA*). For each 20 µl aliquot, the composition of the PCR reaction is shown in Table 4.

Table 4. PCR reaction composition per 20 μ l aliquot.

Reagent	Volume
10X PCR buffer (per 10 ml: 5 ml 1.34 M Tris-HCl, pH 8.8; 1 ml 1.66 M (NH ₄) ₂ SO ₄ ; 1 ml 670 mM MgCl ₂ ; 35.1 μ l 2-mercaptoethanol; 1.34 μ l 0.5 M EDTA, pH 8.0; 1.34 μ l ddH ₂ O)	2 μl
1.6 mg/ml BSA¹ (BSA diluted to 1.6 mg/ml with filter sterilized ddH ₂ O, boiled for 15 min, stored at -20°C)	0.125 μl
dNTP mix (25 mM each: dATP, dCTP, dGTP, dTTP)	1 μl
ddH₂O	13.175 μl
DMSO²	2.5 μl
Taq Polymerase	0.2 μl
Primer 1³ (100 μg/ml)	0.5 μl
Primer 2³ (100 μg/ml)	0.5 μl

¹ Bovine Serum Albumin² Dimethyl Sulfoxide³ Two separate sets of reactions were set up: the first for the wild-type allele, and the second for the mutant allele. Each used the same common primer, as well as a second specific primer for the respective allele.

Separate reactions were carried out for the wild-type and mutant allele, with the common primer 5'-TGA AGG TGG TCT TCA AGA GCA GTC CT-3' (oDT 44) with either 5'-TAT CCT CGG CAG ACC TGA GTC GTG T-3' (oDT 66, primer specific for wild-type allele, ~1.9 kb) or 5'-GAT TGG GAA GAC AAT AGC AGG CAT GC-3' (Si75, primer specific for mutant allele, ~1.4 kb). PCR was started with an initial cycle of denaturation at 94°C for 2 minutes, annealing at 57°C for 2 minutes, and extension at 65°C for 5 minutes. 40 subsequent cycles followed with denaturation at 94°C for 30 seconds, annealing at 57°C for 30 seconds, and extension at 65°C for 90 seconds. Finally, extension was carried out at 65°C for 10 minutes. PCR products were separated on a 1% agarose gel stained with ethidium bromide.

2.2.10 Tissue Collection and Morphometric Analysis of of Aortas and Aortic Sinus

After 12 weeks on the western diet, mice were fasted overnight for 16 hours, and injected with a lethal dose (approximately 0.9 ml) of 2.5% Avertin in PBS. Mice were sprayed down with ethanol and blood was collected by cardiac puncture for plasma analysis (see 2.2.3. *Collection of Blood*).

An incision was made in the lower abdomen, cutting through the peritoneum and then up towards the thorax. The rib cage was opened and skin flaps pinned down. The circulatory system was perfused with approximately 10 ml PBS containing 1 mM EDTA (4°C, pH 8.0) via a winged butterfly needle (23G x 0.75" needle, 12", 0.4 ml tubing,

Terumo Medical Corporation) inserted into the apex of the heart, and a plunger-less 30 ml syringe as the fluid reservoir. After perfusion was seen to be complete (indicated by pallor of organs such as the liver, lungs, and kidneys), the lungs and all abdominal organs obliterating the view of the aorta were removed. The diaphragm was cut down to the posterior abdominal wall. Iliac arteries were cut distal to the iliac bifurcation, and the aorta was pulled up and slowly removed by cutting it away posteriorly, close to the spine, moving superiorly. After cutting up to the level of the diaphragm, carotid arteries were dissected out and severed from the neck. Dissection of the aorta from the spine was now continued from the level of the arch moving inferiorly until completely detached [Tangirala RK *et al*, 1995].

Aortas were then placed under a dissecting microscope and dissected partially free of fat and extraneous tissues. The point of branching of the brachiocephalic and carotid arteries was located, and the aorta was cut proximal to the emergence of these branches. Aortas were placed in 10% formaldehyde solution for approximately 3 days. Subsequently, they were removed, rinsed with distilled water, and placed on a tissue culture plate. Under a dissecting microscope, they were dissected free of all extraneous tissue and adventitious fat. To keep aortas moist during this time, they were frequently dipped in distilled water. After clearing most fat and extraneous tissue, a razor blade was used to cut off vascular branches. Aortas were then rinsed in distilled water, placed in a scintillation vial with 70% ethanol for 30 seconds, and then in another vial with Sudan IV solution (0.5 g Sudan IV, 36.8 ml 95% ethanol, 50 ml acetone, 13.2 ml ddH₂O), to stain lipid-rich areas red, for 15 minutes on a shaking tray. On removal, aortas were placed in a

scintillation vial with 80% ethanol for one minute to remove excess Sudan IV, and rinsed in distilled water. They were then placed again under a dissecting microscope to remove any extraneous fat that may have been left, now seen as stained red. A single aorta was now placed on a superfrost plus microscope slide (VWR Canlab, Catalog # 48323-185) and longitudinally cut open using dissecting microscissors (Roboz Surgical Instrument Co., Inc.) with a 5 mm blade. Aortas were opened and mounted onto slides using glycerol-gelatin (59% w/v glycerol, 0.9% w/v gelatin, 1% w/v phenol) pre-warmed to 55°C. Each aorta was held open on the slide using blunt-ended pins, until the glycerol-gelatin had cooled and held the open aorta in place [Tangirala RK *et al*, 1995]. Slides were allowed to set overnight; all slides were digitally photographed by Tomas Baumgartner, using a Canon D60 digital camera under identical lighting and magnification conditions.

Lipid-rich lesion areas were quantified using Axiovision 3.1 software (Carl Zeiss Vision). Aorta images were divided into 10 equal segments starting from the most superior part of the arch down to the iliac bifurcation. The extent of atherosclerosis was determined morphometrically via Axiovision 3.1 software (using the outline spline tool) as the ratio of the area of lipid-rich Sudan IV stained plaque in the total aorta or given segment to the total area of the aorta or given segment for each mouse.

Hearts were cut at the atrioventricular plane and both portions of each heart were embedded in frozen specimen embedding medium containing 10% polyvinyl alcohol and 4% polyethylene glycol (cryomatrix), placed in a dry ice / 2-methylbutane bath and subsequently stored at -80°C.

Using a cryotome, cross sections of hearts were collected. Approximately 120 10 μm frozen cross sections from the aortic sinus were collected onto slides, starting at the level of the aortic root and moving distally (four sections per slide). Slides were fixed in 37% formaldehyde solution for 1 minute, washed with tap water 7 times, and then stained in a working solution of Oil Red O [96 ml Oil Red O stock (2.5 g Oil Red O, 500 ml isopropanol), 64 ml ddH₂O], to stain lipids red, for 15 minutes. Slides were then washed 2 times with tap water, and stained for 5 minutes in Mayer's Hematoxylin for nuclear staining. Following this, they were washed twice with tap water, once with distilled water, and covered with a layer of Aquaperm mounting medium. They were left to dry overnight, and imaged the next day using a Zeiss Axiovert 200M inverted microscope at 5x magnification. Lesion area quantitation for plaques was carried out morphometrically using the outline spline tool in Axiovision 3.1 software. Total lesion area was determined as the sum of all lesion area values from one cross section. The distance in μm from the aortic root was plotted against mean lesion area for the experimental and control groups, and statistical analysis was carried out using a T-test. The section at the aortic root showing all three valve leaflets was assigned the first section, at a distance of 0 μm , and serial sections were quantitated at 80 μm intervals from here, moving distally.

3. Results

3.1 Conditions for Bone Marrow Transplantation and Repopulation

In order to establish conditions for bone marrow transplantation, I carried out a series of control experiments together with Scott Covey, a colleague in the laboratory. We reasoned that a facile method to assess bone marrow repopulation in transplanted mice would be to use bone marrow from marked donors. We chose GFP-transgenic mouse donors in which GFP (driven by the chicken β actin promoter) is expressed in all tissues and cells except erythrocytes and hair follicles [Okabe M *et al*, 1997]. We decided that this would enable us to easily follow the fate of GFP-tagged donor derived cells in non-transgenic recipient bone marrow transplanted mice.

The first experiment towards this goal involved analyzing blood samples from 2 control mice, one GFP transgenic, and the other non-GFP transgenic. Blood from these mice was collected into heparinized tubes by tail vein bleeding, and erythrocytes were lysed using ammonium chloride. Two blood samples from each were used, where one sample was labelled with a biotinylated anti-CD11b (Mac-1) antibody and a secondary reagent consisting of Cy-Chrome conjugated to streptavidin, and the other was not. In all experiments, cells were analyzed by flow cytometry for GFP and cychrome fluorescence by Hong Liang at the Flow Cytometry Facility at the McMaster University Health Sciences Center, and results were analyzed by WinMDI 2.8 software.

Figure 1 shows results of flow cytometric analysis of blood cells from GFP transgenic (B and D) or control mice (A and C) labelled with anti-CD11b antibody (C,D) or unlabelled (A,B). Each dot represents an individual cell, and fluorescence is measured for both GFP and Cy-Chrome in relative fluorescence units (rfu).

Table 5 shows the number of cells counted in each quadrant of each panel of Figure 1. In samples from GFP transgenic mice also labelled with CD11b antibody, the percentage of CD11b expressing cells also expressing GFP was determined by calculating the proportion of cells in the upper right quadrant as a percentage of the total number of cells in the upper left and upper right quadrants. In the case of this control experiment, 93.2% of all cells expressing CD11b were also GFP transgenic. This value was used as a reference for subsequent bone marrow transplantation experiments that tested the extent of repopulation using these flow cytometry analysis conditions.

Based on these results, bone marrow transplants were carried out on 2 ApoE ^{-/-} mice with donor mice positive for green fluorescence protein (GFP) and recipients negative for GFP, with the objective of testing the proportion of circulating CD11b⁺ cells (including monocytes) that were donor bone marrow derived (GFP⁺). This would give us an idea of the extent of bone marrow repopulation we could expect in our experiments.

Irradiation of these mice was carried out using a Co-60 source at a dose of 1200 cGy split into doses of 800 cGy and 400 cGy three hours apart. Bone marrow harvested from GFP positive donors was transplanted into the GFP negative recipients (*Materials and Methods, 2.2.5. Bone Marrow Transplantation*). For the first two weeks after transplantation, mice were given trimethaprim-sulfamethoxazole in water (6.25 ml of 40

mg/ml trimethaprim and 8 mg/ml sulfamethoxazole 200ml water at a final concentration of 1.25 mg/ml trimethaprim and 0.25 mg/ml sulfamethoxazole), dry pelleted food, powdered food and NutriCal supplement paste saturated in water (containing trimethaprim-sulfamethoxazole at the concentrations above), and daily intraperitoneal injections of 0.5 ml Lactated Ringer's Solution.

Five weeks after transplantation, blood from these mice was collected into heparinized tubes by tail vein bleeding, erythrocytes were lysed, and monocytes and macrophages were labelled with a biotinylated anti-CD11b (Mac-1) antibody as well as a secondary reagent consisting Cy-Chrome conjugated to streptavidin, as described. Again, cells were analyzed by flow cytometry for GFP and cyochrome fluorescence (Figure 2). Reconstitution of donor-derived monocytes and macrophages was indicated by the percentage of total CD11b expressing cells also expressing GFP among all CD11b expressing cells. It was seen that over 79% and 89% of CD11b expressing cells were donor derived in each mouse respectively.

We concluded that GFP can be used efficiently as a marker to assess repopulation in bone marrow transplanted mice. Based on these results, these transplantation conditions were applied to further experiments.

Seeing these data, a series of experiments was carried out to assess the effect of various radiation doses on repopulation and mortality, and look for a dose that was lethal, yet allowed adequate repopulation of donor-derived cells. In the first of these experiments, conducted by Scott Covey and myself, four groups of C57Bl/6 ApoE *-/-* mice were administered 600, 800, 1000, and 1200 cGy respectively using the same

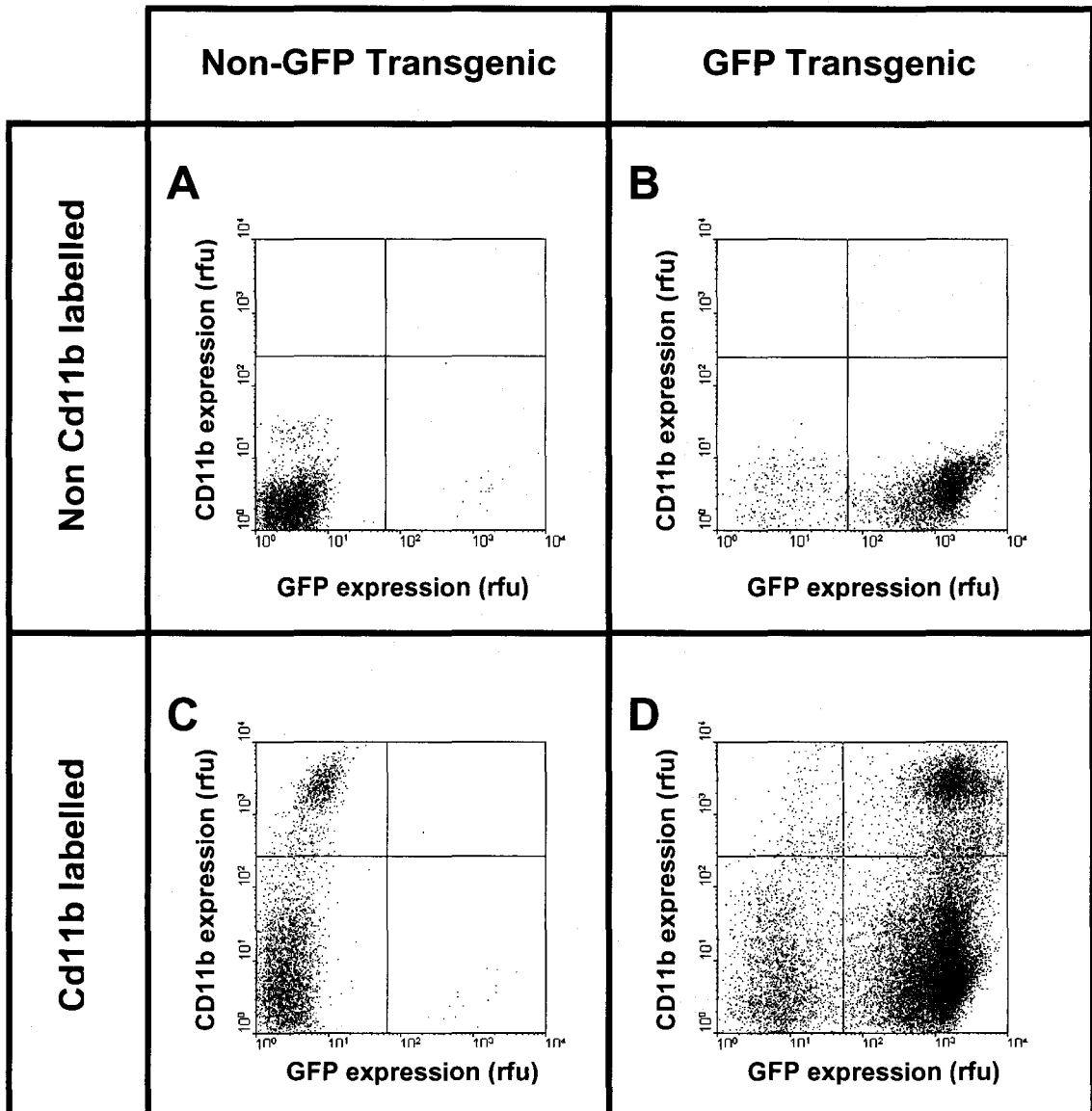


Figure 1. Flow cytometric analysis of GFP and CD11b expression in blood cells. Blood was collected from non-GFP transgenic control (A,C) or GFP transgenic mice (B,D) as described in Materials and Methods (2.2.3. *Collection of Blood*). Red blood cells were lysed and white blood cells were either unlabelled (A,B) or labelled (C,D) with a biotinylated anti-CD11b antibody and Cy-Chrome (Pharmingen)-conjugated streptavidin in the presence of Fc block⁴, as described in Materials and Methods (2.2.8. *Flow Cytometric Analysis of Blood Cells*). CD11b expression (relative Cy-Chrome fluorescence units, rfu) is plotted on the vertical axis, and GFP expression (rfu) is plotted on the horizontal axis for each cell analyzed (each dot corresponds to an individual cell) by flow cytometry. The horizontal lines in each panel separate cells with low (lower quadrants) and high (higher quadrants) CD11b expression. The vertical lines in each panel separate cells with low (left quadrants) and high (right quadrants) GFP expression and were placed based on panels A, B, and C.

⁴ See Materials and Methods, 2.2.7. *Flow Cytometric Analysis of Blood Cells*

Table 5. Flow cytometric analysis of blood cells from non-transgenic and GFP-transgenic mice.

Panel ^a	Number of Cells in Quadrant				Total	UR vs U (%) ^b
	Upper Left	Upper Right	Lower Left	Lower Right		
A	0	1	3911	17	3929	NA
B	0	0	303	3610	3913	NA
C	950	0	2981	13	3944	NA
D	361	4952	2165	16347	23825	93.2

^apanel in Figure 1

^bpercentage of cells in upper right quadrant versus upper right and upper left

NA: not applicable

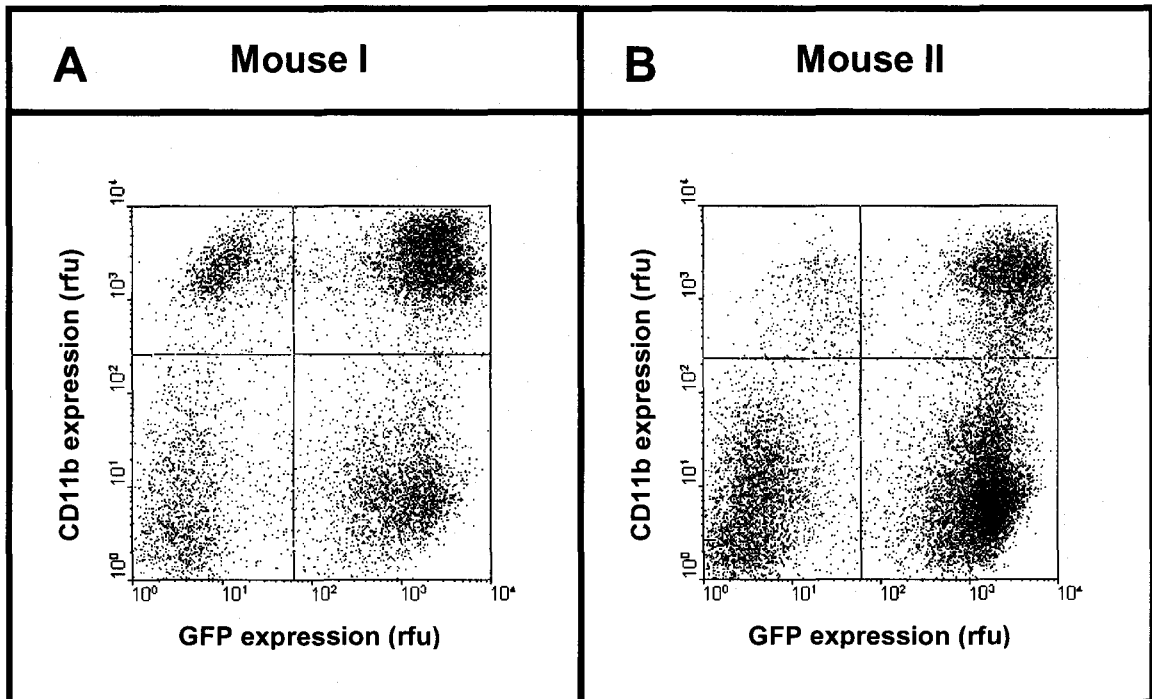


Figure 2. Flow cytometric analysis of blood cells after bone marrow transplantation. ApoE $-/-$ mice were irradiated with a dose of 1200 cGy using a cobalt (Co-60) source, and transplanted with $\sim 2.5 \times 10^6$ bone marrow cells from an ApoE $-/-$ GFP transgenic donor. One month after transplantation, blood was collected into heparinized tubes via tail vein bleeding (*Materials and Methods, 2.2.3. Collection of Blood*). 30 μ l of whole blood was treated with NH_4Cl to lyse erythrocytes, and white blood cells were washed and labelled with biotinylated anti-CD11b antibody and Cy-Chrome (Pharmingen)-conjugated streptavidin in the presence of Fc block (*Materials and Methods, 2.2.8. Flow Cytometric Analysis of Blood Cells*). Cells were subjected to 2 color flow cytometry. Cy-Chrome fluorescence, indicating CD11b expression (relative Cy-Chrome fluorescence units, rfu) is on the vertical axis, and GFP fluorescence (relative fluorescence units, rfu) is on the horizontal axis (see *Materials and Methods, 2.2.8. Flow Cytometric Analysis of Blood Cells* for excitation and emission wavelengths). The boundaries of quadrants were set based on the data from Figure 1. Cells in the upper quadrants have high levels of CD11b expression (monocytes and dendritic cells), and cells in the right quadrants have high levels of GFP expression and are therefore donor derived. Repopulation was assessed by determining the proportion of CD11b $^+$ cells that were also GFP $^+$ according to the formula $\text{UR}/(\text{UR}+\text{UL})$. For Mouse I (A), 79% of CD11b $^+$ cells were donor derived, and for Mouse 2 (B), 89% of CD11b $^+$ cells were donor derived.

conditions described above, except the first dose was 600 cGy, and the second dose, administered three hours later, was either 0, 200, 400, or 600 cGy. Mice were transplanted with bone marrow from GFP transgenic mice. Like the previous repopulation assessment experiment, five weeks after transplantation, blood from mice was collected in heparinized tubes, erythrocytes lysed, and monocytes labelled with a biotinylated anti-CD11b (Mac-1) antibody and the secondary reagent consisting of Cy-Chrome conjugated to streptavidin. Flow cytometric analysis of cells from control GFP transgenic and non-GFP transgenic mice was carried out in the same way as shown in Figure 1 (data not shown).

In Figure 3, results are shown for individual representative mice from each dosage group. Collectively, the upper quadrants represent cells expressing CD11b (including monocytes), and repopulation is calculated by determining the percentage of CD11b expressing cells also expressing GFP (upper right quadrant) among all of the cells expressing CD11b (upper right and upper left quadrants). These percentages are shown in Table 6 for each mouse in the experiment.

All mice showed efficient repopulation, (mean for all groups ~95%, range 89-99%) including those that received lower radiation dosages. For each radiation group, one mouse served as an irradiation control that was irradiated but did not receive bone marrow. Out of these control mice, only the one in the 600 cGy dosage group survived the 2 week period following irradiation, indicating that this dosage was sub-lethal. All transplanted mice in the experiment survived.

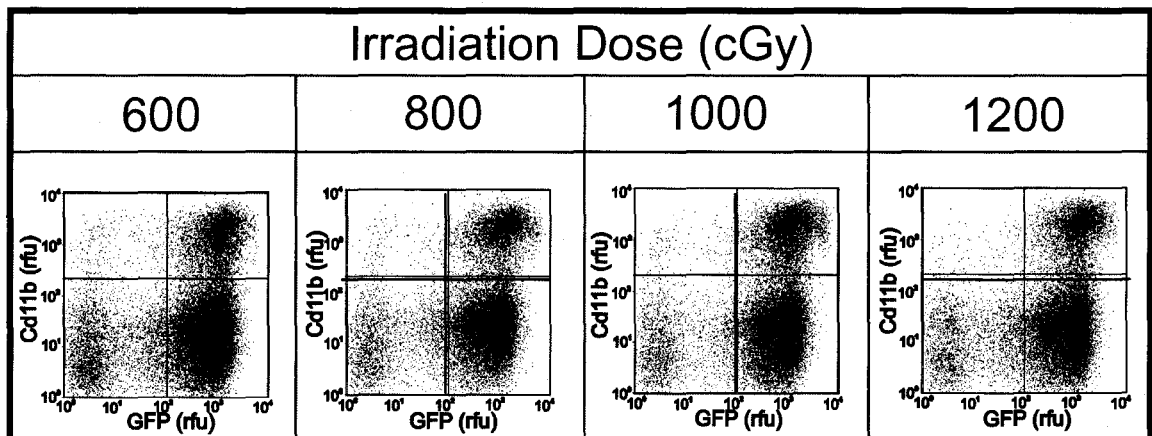


Figure 3. Effect of radiation dose on bone marrow repopulation. 2 or 3 ApoE^{-/-} recipient mice were exposed to a total of either 600, 800, 1000, or 1200 cGy using a Co-60 irradiation source. The total dose was split into 2 doses: 600 cGy was given as the first dose and then either 0, 200, 400, or 600 cGy 3 hours later. Bone marrow cells ($\sim 2 \times 10^6$) from ApoE^{-/-} GFP transgenic donor mice were injected into irradiated recipients intravenously and mice were housed in the Central Animal Facility at McMaster University (*Materials and Methods*, 2.2.1 *Generation and Maintenance of Mice*; 2.2.5. *Bone Marrow Transplantation*). One month after transplantation, heparinized blood was collected via tail vein bleeding (*Materials and Methods*, 2.2.3. *Collection of Blood*), red blood cells were lysed, and white blood cells were labelled with a biotinylated anti-CD11b antibody and Cy-Chrome (Pharmingen)-conjugated streptavidin. Cells were analyzed by flow cytometry as described in the legend to Figure 1 (*Materials and Methods*, 2.2.8. *Flow Cytometric Analysis of Blood Cells*). The degree of donor repopulation was determined as described in the legend to Figure 2. Representative plots are shown. Boundaries of quadrants were determined based on data from non-GFP transgenic and GFP transgenic controls either labelled or unlabelled with CD11b, similar to Figure 1 (not shown). Extents of repopulation are shown in Table 6.

Table 6. Effect of radiation dose on bone marrow repopulation.

Irradiation (cGy)	Lethal Dose ^a	UL+UR ^b	UR ^c	UR/(UL+UR) % ^d	Average (%)
600	no	7012	6737	96	93 ± 6 ^e
		6691	6010	90	
800	yes	6538	6280	96	93 ± 6 ^e
		6652	5974	89	
1000	yes	7362	7264	98	98 ± 1 ^f
		5119	5027	98	
		6518	6305	97	
1200	yes	5815	5741	99	97 ± 3 ^e
		6956	6681	96	

^a Lethal dose: death within 14 days of irradiation in mice not receiving donor bone marrow

^b cells in upper left and upper right quadrants

^c cells in upper right quadrant

^d percentage of cells in upper right versus upper left and upper right quadrants

^e difference between repopulation of 2 mice

^f standard deviation

In subsequent transplantation experiments, post-transplantation mortality was unacceptably high. At this point, we decided to change other factors apart from radiation dosage in an attempt to rescue the raised post-transplantation mortality rate. These changes were based on literature, results from past experiments, and information gathered from autopsy reports of dead mice. Here on, recipient mice were transplanted at 12 weeks of age instead of 6 weeks, and were given bone marrow cells harvested under sterile conditions and filtered through a 100 μ m cell strainer. The dose of radiation was reduced to 900 cGy, and trimethaprim-sulfamethoxazole was administered via Jell-O (5-7 ml Jell-O per day, 1.25-0.25 mg/ml final concentration) in addition to drinking water with the same final concentration of trimethaprim-sulfamethoxazole. Intra-peritoneal fluid injections were also stopped, and only given when mice showed signs of moderate to severe dehydration. Mice transplanted under these revised conditions showed almost 100% post-transplantation survival, and PCR analysis of blood (see below) demonstrated efficient repopulation.

3.2 PCR to Test for Repopulation

For the previous experiments, I had used GFP transgenic donors and non-GFP transgenic recipients to quantitatively assess bone marrow repopulation. For the transplantation experiments required for the project, I used SR-BI $+/+$ ApoE $-/-$ and SR-BI $-/-$ ApoE $-/-$ donors to transplant cells into ApoE $-/-$ recipients that had a defined C57Bl/6 genetic background. Due to the unavailability of SR-BI/ApoE double knockout

mice that were also GFP transgenic, we proceeded with the non-GFP transgenic mice that were available to us and used a qualitative PCR test to check for repopulation.

Four and one-half weeks after transplantation, blood samples were drawn from the tail veins of mice into heparinized tubes, and DNA was isolated using a NucleoSpin Blood Quick Pure Mini kit. Genotyping of the SR-BI locus was carried out via PCR, using separate reactions for the wild-type and mutant alleles (see Materials and Methods, 2.2.9. *PCR Genotyping*).

In Figure 4, lanes 1-6 show PCR genotyping results from tail-derived DNA as controls. Lanes 1 and 2 show SR-BI $+/+$ tail DNA, with detection of the wild type allele only. Lanes 3 and 4 show SR-BI $+/-$ DNA, with bands for both the wild-type and mutant SR-BI alleles, and lanes 5 and 6 show SR-BI $-/-$ DNA with only the mutant allele detected. Blood cell DNA from chimeric mice is shown in the panel on the right in two mice transplanted with SR-BI $-/-$ bone marrow and one mouse transplanted with SR-BI $+/+$ DNA. Lanes 7 and 8 show the results of one of the mice that received SR-BI $-/-$ bone marrow with successful repopulation as signified by a clear band in the reaction for the mutant allele (lane 8) and the absence of a product in the reaction for the wild-type allele (lane 7). The second mouse, (lanes 9 and 10) is an example of inadequate repopulation, showing both wild-type and mutant alleles. The PCR results for this mouse are not as clear, but are reported and shown here as an example of one of two mice in the entire study that showed incomplete repopulation. These mice were excluded from the study. In the blood from a mouse that received SR-BI $+/+$ bone marrow (lanes 11 and 12), only the wild-type allele is seen on PCR analysis as expected.

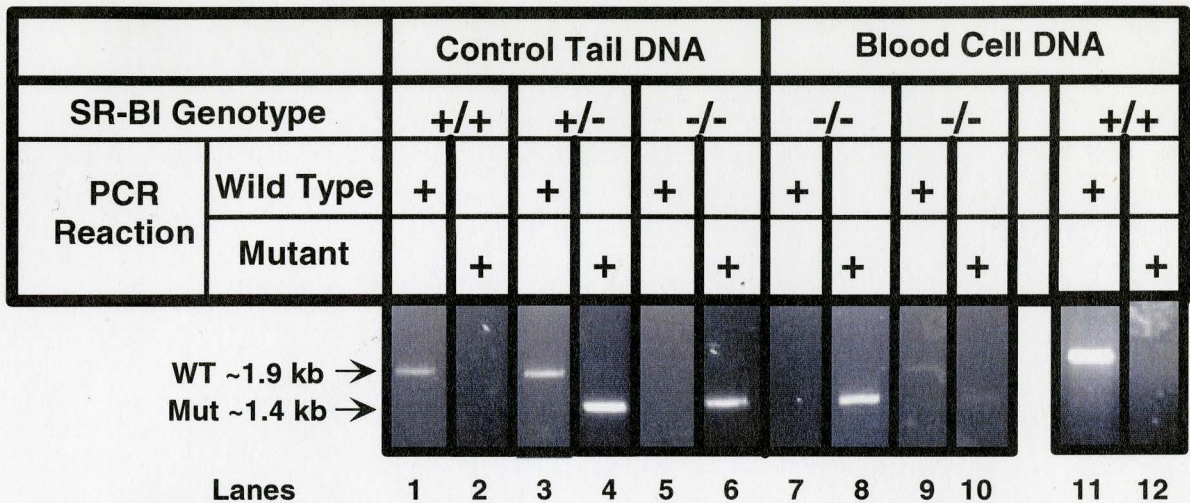


Figure 4. PCR genotyping analysis of blood cells after bone marrow transplantation for repopulation assessment. One month after bone marrow transplantation, blood was collected from mice in heparinized tubes by tail vein bleeding (*Materials and Methods, 2.2.3. Collection of Blood*). DNA from blood was prepared using a Nucleospin Quick Pure Mini kit (BD Biosciences), and PCR analysis was carried out using primers to detect either the SR-BI $+/+$ or SR-BI $-/-$ allele (*Materials and Methods, 2.2.7. Preparation of Blood Cell DNA; 2.2.9. PCR Genotyping*). Lanes 1-6 represent PCR analysis of tail-derived DNA from controls of the specified genotype. Lanes 7-12 show results of PCR of blood cell DNA from mice transplanted with either SR-BI $+/+$ (lanes 11, 12) or SR-BI $-/-$ (lanes 7-10) donor bone marrow. Lanes 1, 3, 5, 7, 9, and 11 correspond to the wild-type PCR reaction; wild-type PCR product has a size of ~1.9 kb as indicated. Lanes 2, 4, 6, 8, 10, and 12 correspond to the mutant-specific PCR reaction; mutant PCR product is ~1.4 kb as indicated. Lanes 7 and 8 show the result from the blood cell DNA of an ApoE $-/-$ mouse transplanted with SR-BI $-/-$ ApoE $-/-$ bone marrow. The presence of the mutant allele in the absence of the wild-type allele indicates efficient repopulation. Lanes 9 and 10 show the result from another ApoE $-/-$ mouse transplanted with SR-BI $-/-$ ApoE $-/-$ bone marrow with presence of both wild-type and mutant alleles, indicating partial repopulation. This mouse was excluded from the study. Lanes 11 and 12 show the result from an ApoE $-/-$ mouse transplanted with SR-BI $+/+$ ApoE $-/-$ bone marrow, with only the wild-type allele detected.

3.3 Analysis of Plasma Cholesterol Levels and Lipoprotein Profiles

To look for the effects of selective SR-BI expression in bone marrow derived cells on lipoprotein and cholesterol metabolism, plasma from transplanted mice in both groups was analyzed for total cholesterol levels and distribution among lipoproteins.

Figure 5 shows total plasma cholesterol levels in ApoE^{-/-} mice transplanted with SR-BI^{+/+} ApoE^{-/-} or SR-BI^{-/-} ApoE^{-/-} bone marrow cells. One month after transplantation, mice on normal chow transplanted with SR-BI^{+/+} ApoE^{-/-} bone marrow had 435.7 ± 113.3 mg/dl total plasma cholesterol (average \pm standard deviation of 3 determinations: 2 independent pools of plasma with 4 mice/pool and 1 additional mouse), and mice transplanted with SR-BI^{-/-} ApoE^{-/-} bone marrow had 336.1 ± 83.4 mg/dl total plasma cholesterol (average \pm standard deviation of 4 determinations: 2 individual mice and 2 pools of 4 mice and 2 mice). This result was shown not to be statistically significant ($p=0.1$). As mentioned in Materials and Methods, 2.2.6. *Induction of Atherosclerosis*, beginning one month after transplantation, mice were either maintained for 12 weeks on a normal chow diet (preliminary experiment involving 3 mice), or on a high fat diet. Total plasma cholesterol levels for mice maintained a further 12 weeks on normal chow were similar to values measured 1 month post-transplantation: 362 mg/dl ($n=1$) for ApoE^{-/-} mice reconstituted with control SR-BI^{+/+} ApoE^{-/-} bone marrow, and 363 mg/dl ($n=2$) for mice reconstituted with SR-BI^{-/-} ApoE^{-/-} bone marrow. In contrast, mice fed a high fat diet beginning 1 month post-transplantation and continuing for 12 weeks had almost twice as much plasma cholesterol as chow fed mice (Figure 5): $737 \pm$

61 mg/dl (average \pm standard deviation of 3 determinations: 2 independent pools of plasma with 4 mice/pool and 1 additional mouse) and 714 ± 365 mg/dl (average \pm standard deviation of 4 determinations: 1 individual mouse and 3 pools of plasma with 2-4 mice/pool) for mice transplanted with SR-BI $+/+$ ApoE $-/-$ and SR-BI $-/-$ ApoE $-/-$ bone marrow respectively. Bone marrow specific SR-BI elimination had no statistically significant effect on total cholesterol levels in plasma from mice fed a high fat diet ($p=0.5$)

Figure 6 shows lipoprotein profiles from pooled plasma of groups of mice transplanted with SR-BI $-/-$ ApoE $-/-$ or SR-BI $+/+$ ApoE $-/-$ bone marrow. Profiles from chow-fed mice are shown in panel A, and from fat-fed mice in panel B. Peaks for VLDL-sized, IDL/LDL-sized, and HDL-sized lipoproteins were assigned based on analysis of lipoproteins purified from human plasma in our lab [Covey SD *et al*, 2003; Covey SD, Doctoral Thesis, 2003] and by others [Rigotti A *et al*, 1997; Kozarsky KF *et al*, 1997]. Levels of cholesterol associated with different sized lipoproteins were determined by calculating totals across the peaks. Fractions 1-9 represent VLDL-sized lipoproteins, fractions 10-27 represent IDL/LDL-sized lipoproteins, and fractions 30-40 represent HDL-sized lipoproteins.

Figure 7 shows levels of cholesterol associated with VLDL-sized lipoproteins in ApoE $-/-$ mice transplanted with SR-BI $+/+$ ApoE $-/-$ or SR-BI $-/-$ ApoE $-/-$ bone marrow, with 537 ± 143 mg/dl for mice transplanted with SR-BI $+/+$ ApoE $-/-$ bone marrow (average \pm standard deviation of 3 determinations: 2 independent pools of plasma with 2-4 mice/pool and 1 additional mouse), and 494 ± 269 mg/dl for mice transplanted with

SR-BI^{-/-} ApoE^{-/-} bone marrow (average \pm standard deviation of 4 determinations: 3 independent pools of plasma with 2-4 mice/pool and 1 additional mouse). No statistically significant difference was seen between total VLDL-sized lipoprotein cholesterol levels in the two groups ($p = 0.4$).

Figure 8 shows levels of cholesterol associated with IDL/LDL-sized lipoproteins in ApoE^{-/-} mice transplanted with SR-BI^{+/+} ApoE^{-/-} or SR-BI^{-/-} ApoE^{-/-} bone marrow, For the same pools and n values described for cholesterol associated with VLDL-sized lipoproteins, mice transplanted with SR-BI^{+/+} ApoE^{-/-} bone marrow had 244 ± 62 mg/dl and mice transplanted with SR-BI^{-/-} ApoE^{-/-} bone marrow had 224 ± 132 mg/dl cholesterol associated with IDL/LDL-sized lipoproteins. No statistically significant difference was seen between total IDL/LDL-sized lipoprotein cholesterol levels in the two groups ($p = 0.4$). Similar findings for cholesterol levels associated with VLDL- and IDL/LDL-sized lipoproteins were recently reported by Covey *et al* for LDL receptor knockout mice transplanted with either SR-BI^{+/+} or SR-BI^{-/-} bone marrow [Covey SD *et al*, 2003].

Figure 9 shows levels of cholesterol associated with HDL-sized lipoproteins in ApoE^{-/-} mice transplanted with SR-BI^{+/+} ApoE^{-/-} or SR-BI^{-/-} ApoE^{-/-} bone marrow. Interestingly, for the same pools and n values described above, mice transplanted with SR-BI^{-/-} ApoE^{-/-} bone marrow (11 ± 6.6 mg/dl) had significantly decreased levels of cholesterol associated with HDL-sized lipoproteins compared to control mice that received SR-BI^{+/+} ApoE^{-/-} bone marrow (20 ± 1.8 mg/dl, $p=0.035$). This result is in contrast to findings for cholesterol levels associated with HDL-sized lipoproteins

reported by Covey *et al* for LDL receptor knockout mice transplanted with either SR-BI $+/+$ or SR-BI $-/-$ bone marrow [Covey SD *et al*, 2003]. This difference may in part be related to the lack of ApoE in both recipient and donor mice used in this study, and the presence of intact ApoE expression in the mice used in the study by Covey *et al* [Covey SD *et al*, 2003].

Taken together, these results suggest that SR-BI in bone marrow derived cells may have a significant effect on the regulation of HDL cholesterol levels in the absence of ApoE, but not in its presence. To ensure this, the transplantation experiment can be conducted with a higher number of plasma samples from individual mice analyzed for potential differences in HDL cholesterol levels. Also, recipients can be transplanted with SR-BI $+/+$ or SR-BI $-/-$ bone marrow cells with intact ApoE gene expression.

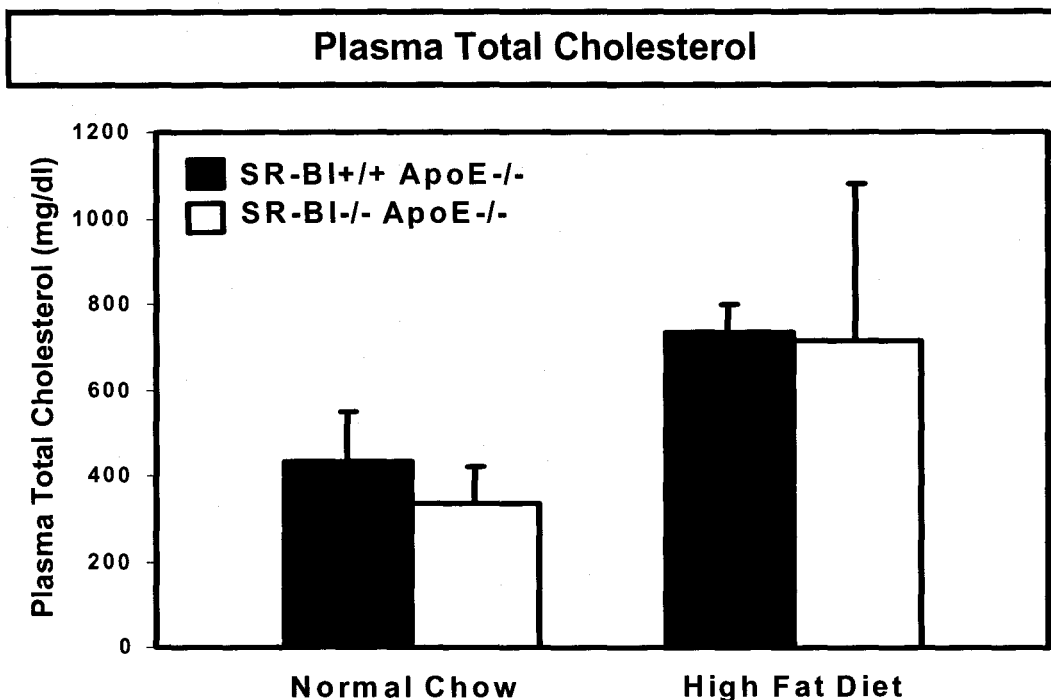


Figure 5. Plasma total cholesterol in ApoE^{-/-} mice transplanted with SR-BI^{+/+} ApoE^{-/-} or SR-BI^{-/-} ApoE^{-/-} bone marrow. ApoE^{-/-} mice were transplanted with either SR-BI^{+/+} ApoE^{-/-} or SR-BI^{-/-} ApoE^{-/-} bone marrow, blood was collected from mice 4 weeks after transplantation, prior to placing them on a high fat diet (left, Normal Chow) and after the subsequent 12 weeks on the high fat diet (right, High Fat Diet). Plasma was prepared from blood samples (*Materials and Methods*, 2.2.3. *Collection of Blood*), and comparison of plasma total cholesterol levels between the two groups was carried out using the Infinity Cholesterol Liquid Stable Reagent Kit (ThermoDMA; *Materials and Methods*, 2.2.4. *Preparation of Plasma and Analysis of Plasma and Lipoprotein Cholesterol*), both before and after administration of the high fat diet. On normal chow, mice transplanted with SR-BI^{+/+} ApoE^{-/-} bone marrow had 435.7 ± 113.3 mg/dl total plasma cholesterol (average ± standard deviation of 3 determinations: 2 independent pools of plasma with 4 mice/pool and 1 additional mouse), and mice transplanted with SR-BI^{-/-} ApoE^{-/-} had 336.1 ± 83.4 mg/dl total plasma cholesterol (average ± standard deviation of 4 determinations: 2 individual mice and 2 pools of 4 mice and 2 mice). After 12 weeks on a high fat diet, mice had 736.9 ± 61 (average ± standard deviation of 3 determinations: 2 independent pools of plasma with 4 mice/pool and 1 additional mouse) and 714 ± 365.4 (average ± standard deviation of 4 determinations: 1 individual mouse and 3 pools of plasma with 2-4 mice/pool) mg/dl respectively for each group. No statistically significant difference was seen between total cholesterol levels in the two groups on normal chow ($p = 0.1$) or on a high fat diet ($p = 0.5$).

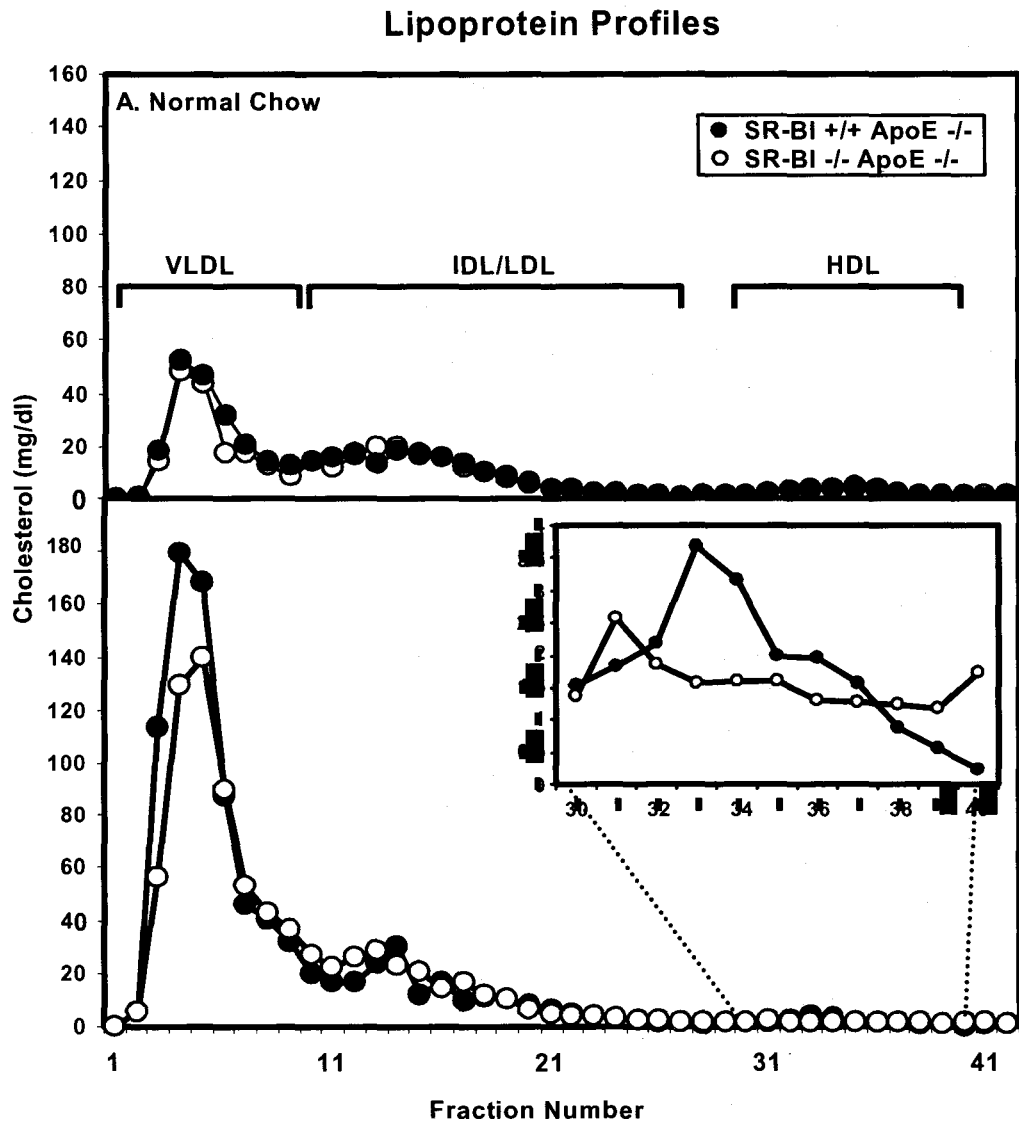


Figure 6. Comparison of plasma lipoprotein profiles 16 weeks post-transplantation in mice that received SR-BI $+/+$ ApoE $-/-$ (closed circles) or SR-BI $-/-$ ApoE $-/-$ (open circles) bone marrow, fed a normal chow (A) or a high fat diet (B). Mice were bled (*Materials and Methods*, 2.2.3. *Collection of Blood*), and plasma was fractionated using an AKTA FPLC with a Superose 6 HR 10/30 column and 154 mM NaCl/1 mM EDTA, pH 8 as the elution solution (*Materials and Methods*, 2.2.4. *Preparation of Plasma and Analysis of Plasma and Lipoprotein Cholesterol*). Fractions 1-9 represent VLDL-sized lipoproteins, 10-27 represent IDL/LDL-sized lipoproteins, and 30-40 represent HDL-sized lipoproteins. Representative profiles are shown for pooled plasma samples from mice in each group. Inset: Profile of HDL-sized lipoproteins in the two groups.

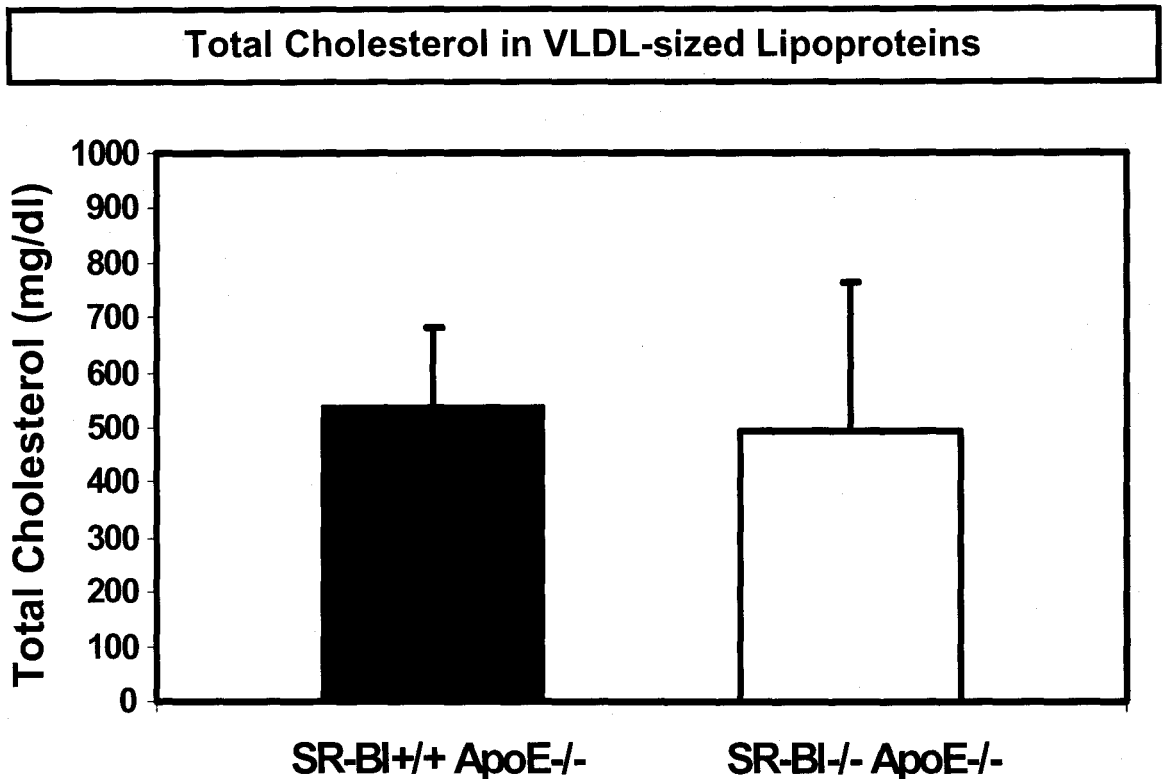


Figure 7. Plasma total cholesterol associated with VLDL-sized lipoproteins in ApoE^{-/-} mice transplanted with SR-BI^{+/+} ApoE^{-/-} (black) or SR-BI^{-/-} ApoE^{-/-} (white) bone marrow. ApoE^{-/-} mice were transplanted with either SR-BI^{+/+} ApoE^{-/-} or SR-BI^{-/-} ApoE^{-/-} bone marrow, blood was collected after 12 weeks on the high fat diet, and plasma was prepared from blood samples (*Materials and Methods, 2.2.3. Collection of Blood*), pooled (for SR-BI^{+/+} ApoE^{-/-} group, average ± standard deviation of 3 determinations: 2 independent pools of plasma with 2-4 mice/pool and 1 additional mouse; for SR-BI^{-/-} ApoE^{-/-} group, average ± standard deviation of 4 determinations: 3 independent pools of plasma with 2-4 mice/pool and 1 additional mouse), and size fractionated as described in the legend to Figure 6. Comparison of VLDL-sized lipoprotein cholesterol levels between the two groups was carried out by assaying Fractions 1-9 using the Infinity Cholesterol Liquid Stable Reagent Kit (ThermoDMA; *Materials and Methods, 2.2.4. Preparation of Plasma and Analysis of Plasma and Lipoprotein Cholesterol*) and adding the total cholesterol values in the fractions. Mice transplanted with SR-BI^{+/+} ApoE^{-/-} bone marrow had 537.0 ± 142.6 mg/dl and mice transplanted with SR-BI^{-/-} ApoE^{-/-} bone marrow had 493.7 ± 268.8 mg/dl total cholesterol associated with VLDL-sized lipoproteins. No statistically significant difference was seen between the two groups (p=0.4).

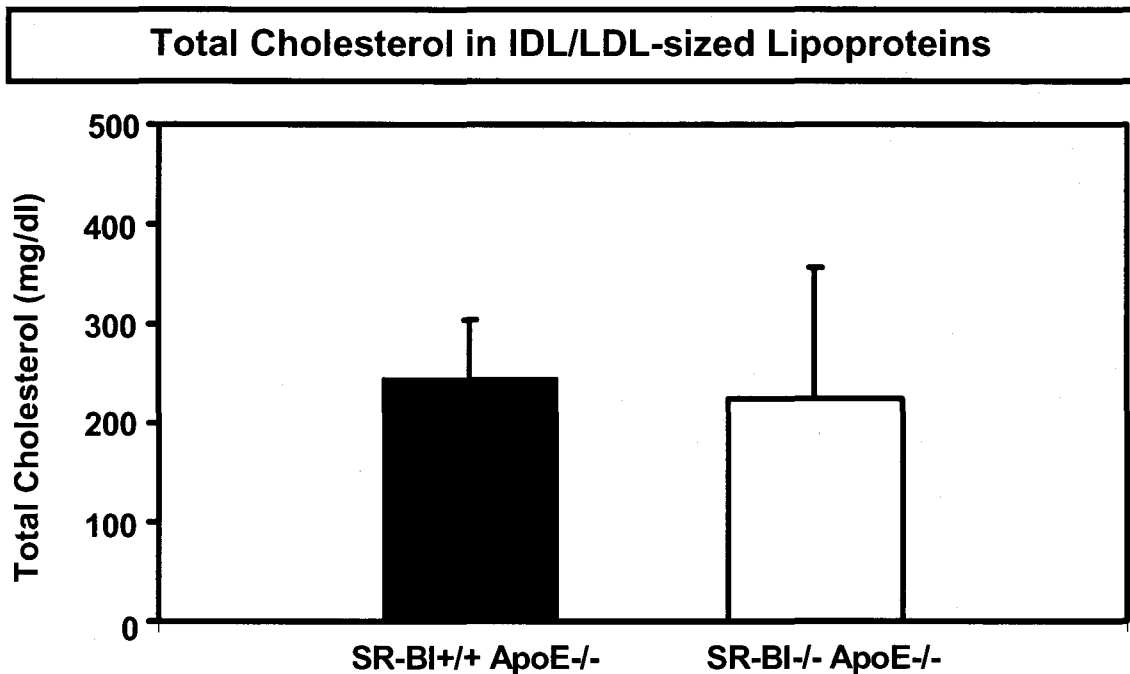


Figure 8. Plasma total cholesterol associated with IDL/LDL-sized lipoproteins in ApoE^{-/-} mice transplanted with SR-BI^{+/+} ApoE^{-/-} (black) or SR-BI^{-/-} ApoE^{-/-} (white) bone marrow. ApoE^{-/-} mice were transplanted with either SR-BI^{+/+} ApoE^{-/-} or SR-BI^{-/-} ApoE^{-/-} bone marrow, blood was collected after 12 weeks on the high fat diet, and plasma was prepared from blood samples (*Materials and Methods, 2.2.3. Collection of Blood*), pooled (for SR-BI^{+/+} ApoE^{-/-} group, average ± standard deviation of 3 determinations: 2 independent pools of plasma with 2-4 mice/pool and 1 additional mouse; for SR-BI^{-/-} ApoE^{-/-} group, average ± standard deviation of 4 determinations: 3 independent pools of plasma with 2-4 mice/pool and 1 additional mouse), and size fractionated as described in the legend to Figure 6. Comparison of IDL/LDL-sized lipoprotein cholesterol levels between the two groups was carried out by assaying Fractions 10-27 using the Infinity Cholesterol Liquid Stable Reagent Kit (ThermoDMA; *Materials and Methods, 2.2.4. Preparation of Plasma and Analysis of Plasma and Lipoprotein Cholesterol*) and adding the total cholesterol values in the fractions. Mice transplanted with SR-BI^{+/+} ApoE^{-/-} bone marrow had 244.1 ± 61.6 mg/dl and mice transplanted with SR-BI^{-/-} ApoE^{-/-} bone marrow had 223.5 ± 132.4 mg/dl total cholesterol associated with IDL/LDL-sized lipoproteins. No statistically significant difference was seen between the two groups (p=0.4).

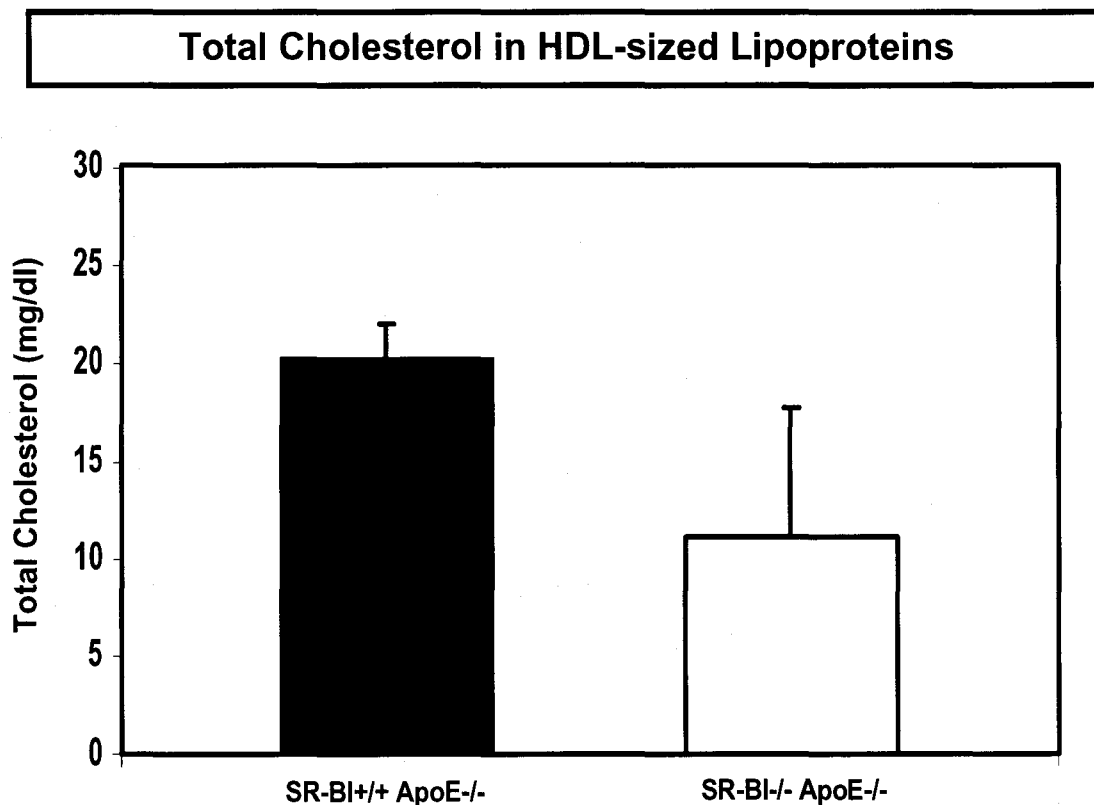


Figure 9. Plasma total cholesterol associated with HDL-sized lipoproteins in ApoE^{-/-} mice transplanted with SR-BI^{+/+} ApoE^{-/-} (black) or SR-BI^{-/-} ApoE^{-/-} (white) bone marrow. ApoE^{-/-} mice were transplanted with either SR-BI^{+/+} ApoE^{-/-} or SR-BI^{-/-} ApoE^{-/-} bone marrow, blood was collected after 12 weeks on the high fat diet, and plasma was prepared from blood samples (*Materials and Methods, 2.2.3. Collection of Blood*), pooled (for SR-BI^{+/+} ApoE^{-/-} group, average ± standard deviation of 3 determinations: 2 independent pools of plasma with 2-4 mice/pool and 1 additional mouse; for SR-BI^{-/-} ApoE^{-/-} group, average ± standard deviation of 4 determinations: 3 independent pools of plasma with 2-4 mice/pool and 1 additional mouse), and size fractionated as described in the legend to Figure 6. Comparison of plasma HDL-sized lipoprotein cholesterol levels between the two groups was carried out by assaying Fractions 30-40 using the Infinity Cholesterol Liquid Stable Reagent Kit (ThermoDMA; *Materials and Methods, 2.2.4. Preparation of Plasma and Analysis of Plasma and Lipoprotein Cholesterol*) and adding the total cholesterol values in the fractions. Mice transplanted with SR-BI^{+/+} ApoE^{-/-} bone marrow had 20.18 ± 1.8 mg/dl and mice transplanted with SR-BI^{-/-} ApoE^{-/-} bone marrow had 11 ± 6.6 mg/dl total cholesterol associated with HDL-sized lipoproteins. Inset: Lipoprotein profiles for HDL-sized particles, fractions 30-40, calculated from this data. The difference between the two groups was found to be statistically significant ($p = 0.035$).

3.4 Histological Assessment of Atherosclerosis Development

To test the effect of selective SR-BI deletion in bone marrow derived cells in ApoE $-/-$ mice, histological assessment of atherosclerosis development was conducted in the two groups. This was done by two methods: first, lipid rich plaque surface area was quantified in aortas of mice as a percentage of the area of the entire aorta, and second, lipid rich plaque areas were quantified for the two groups in cross sections from the aortic roots of mice, expressed as total lesion area per section.

Harvested aortas from mice were fixed in formaldehyde and dissected free of all extraneous tissue and adventitial fat. They were then stained with Sudan IV to color lipids red, and cut open longitudinally. Aortas were mounted onto slides with glycerol-gelatin. Images were captured and analyzed morphometrically. Plaque surface area was determined as a percentage of the total surface area of the entire aorta as well as the thoracic (top $2/5$ of aorta including the arch) and the abdominal (bottom $3/5$ to the iliac bifurcation) aorta (Figure 10). Lipid rich plaque development was mainly seen in the aortic arch and the abdominal aorta. Figure 10 shows images of an aorta from each group. The deep red Sudan IV stained regions represent areas rich in lipids, as indicated by the arrows.

ApoE $-/-$ mice transplanted with SR-BI $-/-$ ApoE $-/-$ bone marrow had ~1.3-fold more atherosclerotic plaque coverage over the entire aorta compared to control mice transplanted with SR-BI $+/+$ ApoE $-/-$ bone marrow (Figure 11; 6.4 ± 2.3 %, $n=9$ and 4.8 ± 0.6 %, $n=8$ respectively, $p=0.03$). The majority of this difference was due to a 2.5-fold

increase in the average amount of atherosclerotic plaque coverage in the abdominal aorta (Figure 13; 4.5 ± 3.2 %, n=9 and 2.0 ± 0.9 %, n=8 respectively, p=0.025). The slight increase in atherosclerotic plaque coverage in the thoracic aorta (Figure 12; 8.5 ± 3.5 %, n=9 and 7.6 ± 1.5 %, n=8 respectively) was not found to be statistically significant (p=0.3).

These data showed that deletion of SR-BI in bone marrow cells of ApoE $-/-$ mice results in a significantly higher amount of lesion area coverage in the abdominal aorta compared to control mice transplanted with SR-BI $+/+$ ApoE $-/-$ bone marrow.

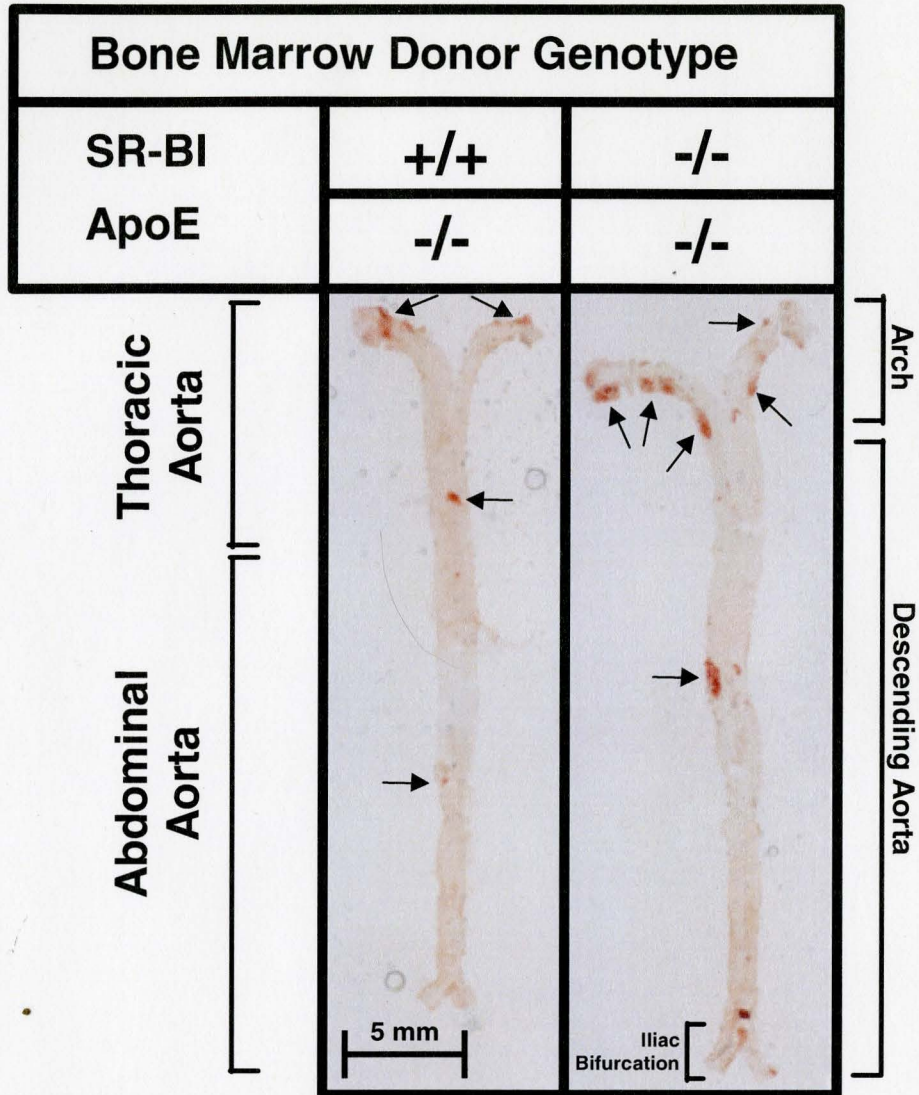


Figure 10. Atherosclerosis in aortas from bone marrow transplanted mice. ApoE $-/-$ mice were transplanted with bone marrow from either SR-BI $+/+$ ApoE $-/-$ control or SR-BI $-/-$ ApoE $-/-$ donor mice. One month after transplantation, mice were fed an atherogenic, high fat western type diet for 12 weeks (*Materials and Methods*, 2.2.6. *Induction of Atherosclerosis*). Mice were euthanized and aortas were harvested and stained for lipid-rich atherosclerotic plaque with Sudan IV. Lipid-rich plaque is indicated by the black arrows. Aortas were mounted on glass slides as described in *Materials and Methods*, and images were captured by Tomas Baumgartner using a Canon D60 digital camera with identical lighting and magnification conditions for each slide (*Materials and Methods*, 2.2.10 *Tissue Collection and Morphometric Analysis of of Aortas and Aortic Sinus*). Representative images are shown. The scale bar corresponds to 5 mm.

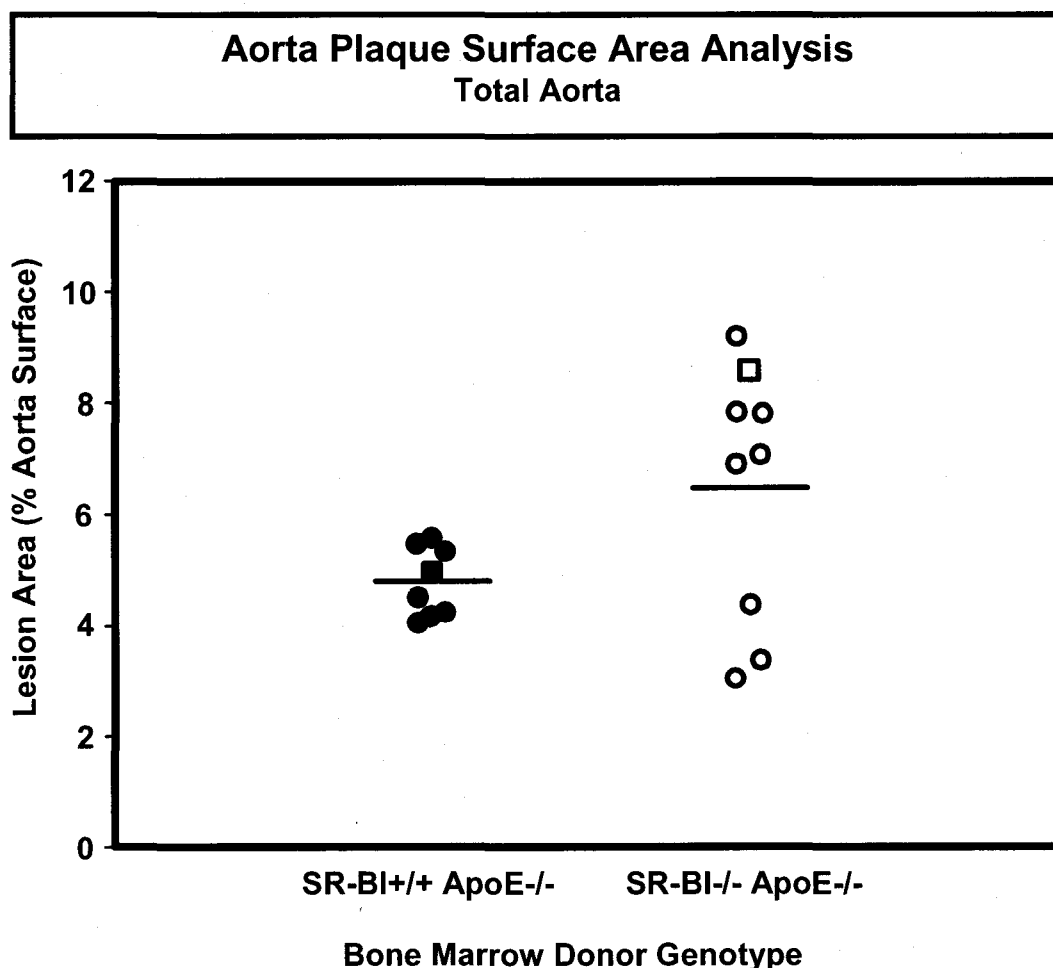


Figure 11. Extent of atherosclerosis in aortas from bone marrow transplanted mice. Atherosclerosis in aortas from mice transplanted with either control SR-BI+/+ ApoE-/- (left) or SR-BI-/- ApoE-/- (right) bone marrow was visualized by Sudan IV staining as described in the legend to Figure 10. The extent of atherosclerosis was determined morphometrically using Axiovision 3.1 software as the ratio of the area of lipid-rich Sudan IV stained plaque to the total area of the aorta for each mouse. The lesion area (expressed as % aorta surface area) is plotted for each mouse. The average lesion areas ($4.8 \pm 0.6\%$, $n=8$ for mice receiving control SR-BI+/+ ApoE-/- bone marrow; $6.4 \pm 2.3\%$, $n=9$ for mice receiving SR-BI-/- ApoE-/- bone marrow) are indicated by the horizontal bars. The square symbols correspond to the aortas shown in Figure 10. Mice receiving SR-BI-/- ApoE-/- bone marrow were seen to have ~35% more atherosclerosis than mice receiving SR-BI+/+ ApoE-/- bone marrow ($p=0.03$).

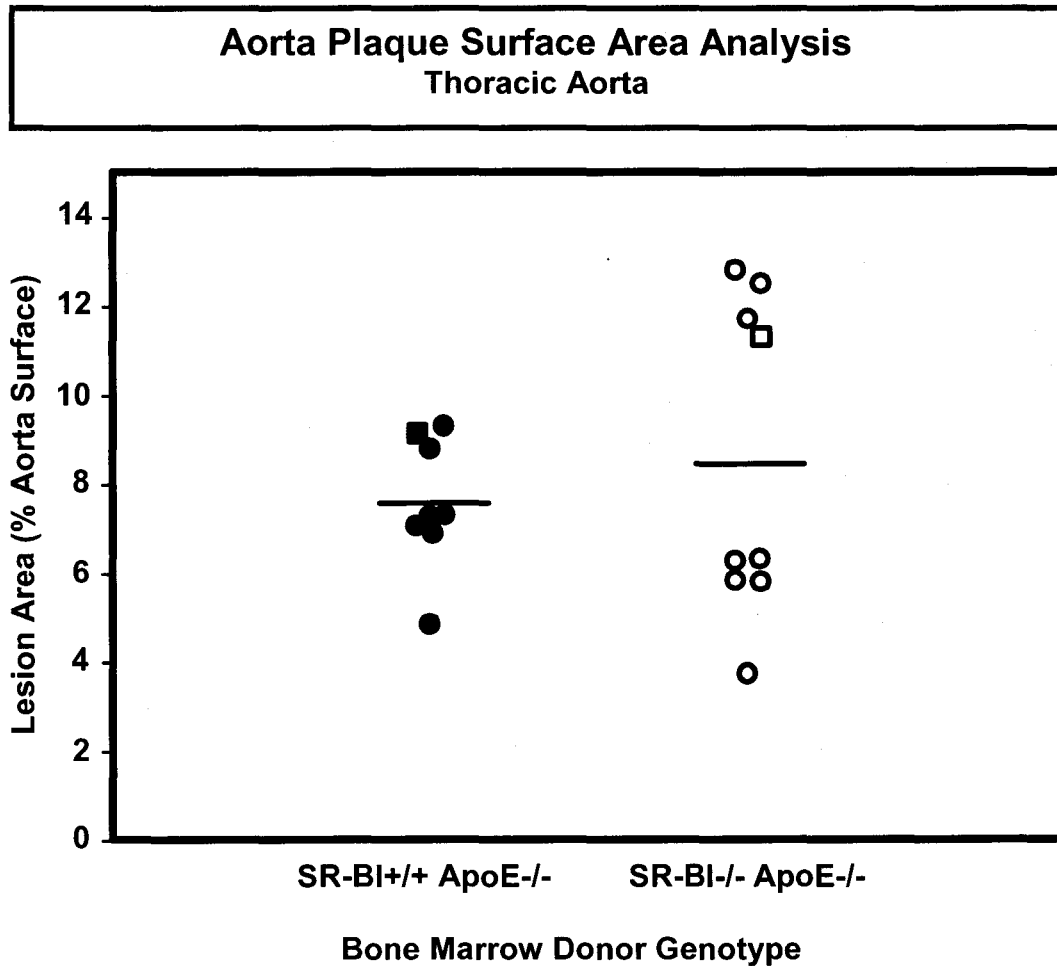


Figure 12. Extent of atherosclerosis in the thoracic aorta from bone marrow transplanted mice. Atherosclerosis in aortas from mice transplanted with either control SR-BI^{+/+} ApoE^{-/-} (left) or SR-BI^{-/-} ApoE^{-/-} (right) bone marrow was visualized by Sudan IV staining as described in the legend to Figure 10. The extent of atherosclerosis was determined morphometrically using Axiovision 3.1 software as the ratio of the area of lipid-rich Sudan IV stained plaque to the total area of the thoracic aorta (Segments 1-4) for each mouse. The lesion area (expressed as % aorta surface area) is plotted for each mouse. The average lesion areas ($7.6 \pm 1.5\%$, $n=8$ for mice receiving control SR-BI^{+/+} ApoE^{-/-} bone marrow; $8.5 \pm 3.5\%$, $n=9$ for mice receiving SR-BI^{-/-} ApoE^{-/-} bone marrow) are indicated by the horizontal bars. The square symbols correspond to the aortas shown in Figure 10. No statistically significant difference in atherosclerosis was seen in aortic arches from mice in the two groups ($p=0.3$).

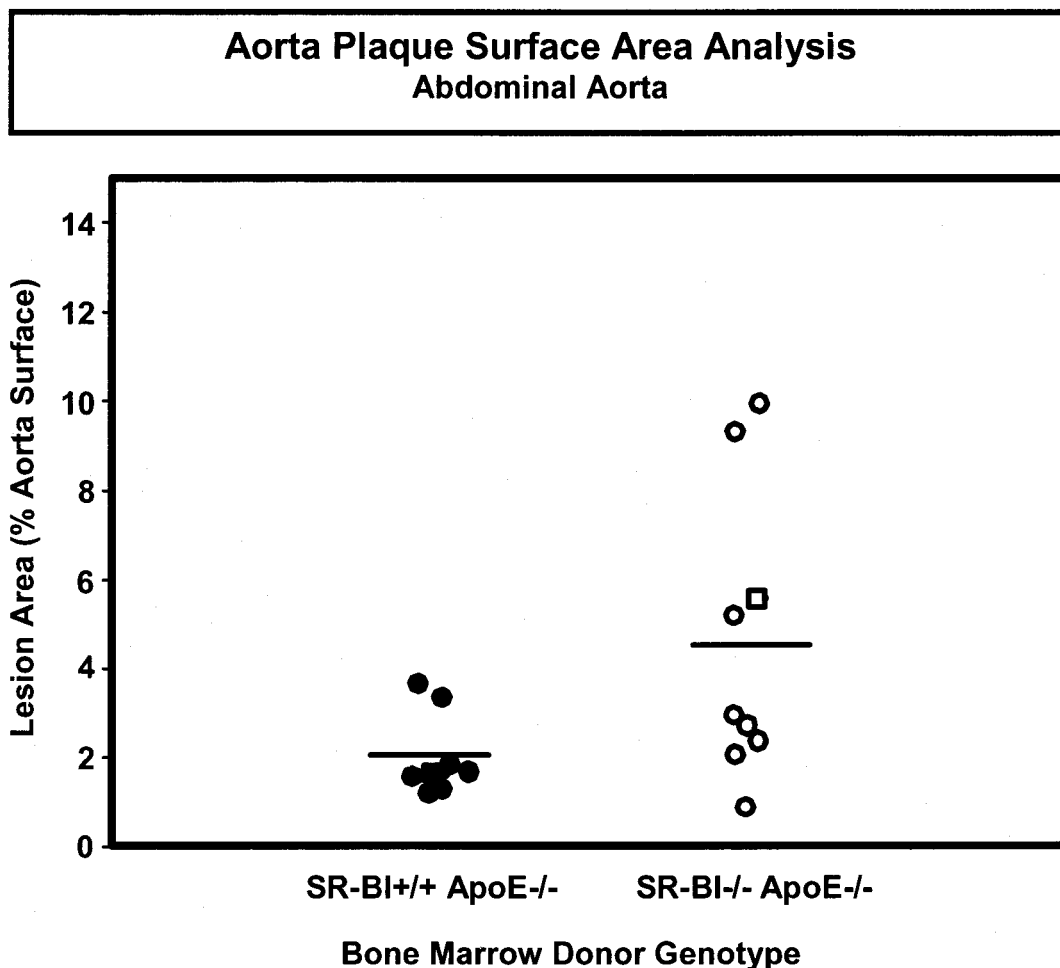


Figure 13. Extent of atherosclerosis in abdominal aortas from bone marrow transplanted mice. Atherosclerosis in aortas from mice transplanted with either control SR-BI^{+/+} ApoE^{-/-} (left) or SR-BI^{-/-} ApoE^{-/-} (right) bone marrow was visualized by Sudan IV staining as described in the legend to Figure 10. The extent of atherosclerosis was determined morphometrically using Axiovision 3.1 software as the ratio of the area of lipid-rich Sudan IV stained plaque to the total area of the abdominal aorta (Segments 5-10) for each mouse. The lesion area (expressed as % aorta surface area) is plotted for each mouse. The average lesion areas (2.0 ± 0.9 %, $n=8$ for mice receiving control SR-BI^{+/+} ApoE^{-/-} bone marrow; 4.5 ± 3.2 %, $n=9$ for mice receiving SR-BI^{-/-} ApoE^{-/-} bone marrow) are indicated by the horizontal bars. The square symbols correspond to the aortas shown in Figure 10. Mice receiving SR-BI^{-/-} ApoE^{-/-} bone marrow were shown to have ~125% more atherosclerosis than mice receiving SR-BI^{+/+} ApoE^{-/-} bone marrow ($p=0.025$).

A second method used to histologically assess atherosclerotic development was the analysis of plaque lesion area in cross sections from the aortic sinuses of mice in both groups. Sections were collected onto slides, fixed with formaldehyde solution, stained with Oil Red O for lipids (red) and Mayer's Hematoxylin for nuclei (blue), and quantitated morphometrically. This assay was used to assess plaque thickness in the aortic root, in contrast to surface area coverage in the aorta as seen in Figures 10-13. Figure 14 shows representative examples from the aortic roots of two mice, one that received SR-BI $+/+$ ApoE $-/-$ bone marrow (A) and one that received SR-BI $-/-$ ApoE $-/-$ bone marrow (B). The aortic root was defined as the cross section at the level of the aortic valves.

Figure 15 shows a comparison of the lesion areas in the aortic roots of mice that that received SR-BI $+/+$ ApoE $-/-$ bone marrow (mean lesion area $288000 \pm 69000 \mu\text{m}^2$) and those that received SR-BI $-/-$ ApoE $-/-$ bone marrow (mean lesion area $311000 \pm 58000 \mu\text{m}^2$). No statistically significant difference was found in the two groups ($p=0.25$).

Seeing no difference in aortic root cross sections between the two groups, I decided to study the distribution of plaque thickness within a 560 μm length of the aortic sinus by quantifying lesion areas in serial cross sections starting at the aortic root and progressing distally. The first section was designated as 0 μm from the aortic root, and subsequent sections were taken serially at distances of 80, 160, 240, 320, 400, 480, and 560 μm from the aortic root. Slides with cross sections were fixed, stained, imaged, and quantified as described above, and the distance from the aortic root was plotted against mean lesion areas for each section, for mice that received either SR-BI $+/+$ ApoE $-/-$ or

SR-BI $-/-$ ApoE $-/-$ bone marrow. Figure 16 shows serial cross section mean lesion areas, beginning with the aortic root (same data as Figure 15), and spaced at 80 μm intervals, plotted vs. the distance from the aortic root for ApoE $-/-$ mice transplanted with either SR-BI $+/+$ ApoE $-/-$ or SR-BI $-/-$ ApoE $-/-$ bone marrow. Both groups showed that plaque cross-sectional area decreased with increasing distance from the aortic root, a trend also demonstrated by others [Caudel T *et al*, 2001]. No significant differences were found for any section level between the two groups ($p > 0.05$).

Cross sections were also analyzed by calculating the total perimeter of the vessel compartment in each section (using Axiovision 3.1 software), and determining what proportion of it was occupied by lipid-rich plaque, as a percentage. No statistically significant differences between percentage perimetric lesion coverage were seen between the two groups ($p > 0.05$). Mice transplanted with SR-BI $+/+$ ApoE $-/-$ bone marrow had an average of 95.7 ± 5.1 % coverage in the 0 μm section and 62.8 ± 21.9 % coverage in the 560 μm section, whereas mice transplanted with SR-BI $-/-$ ApoE $-/-$ bone marrow had an average of 97.6 ± 4.9 % coverage in the 0 μm and 61.2 ± 16.7 % in the 560 μm section (data not shown).

These data showed that there was no difference in either the thickness (atherosclerotic plaque cross-sectional lesion area) or in percentage perimetric lipid rich plaque lesion coverage in mice transplanted with SR-BI $-/-$ ApoE $-/-$ bone marrow compared to control mice transplanted with SR-BI $+/+$ ApoE $-/-$ bone marrow.

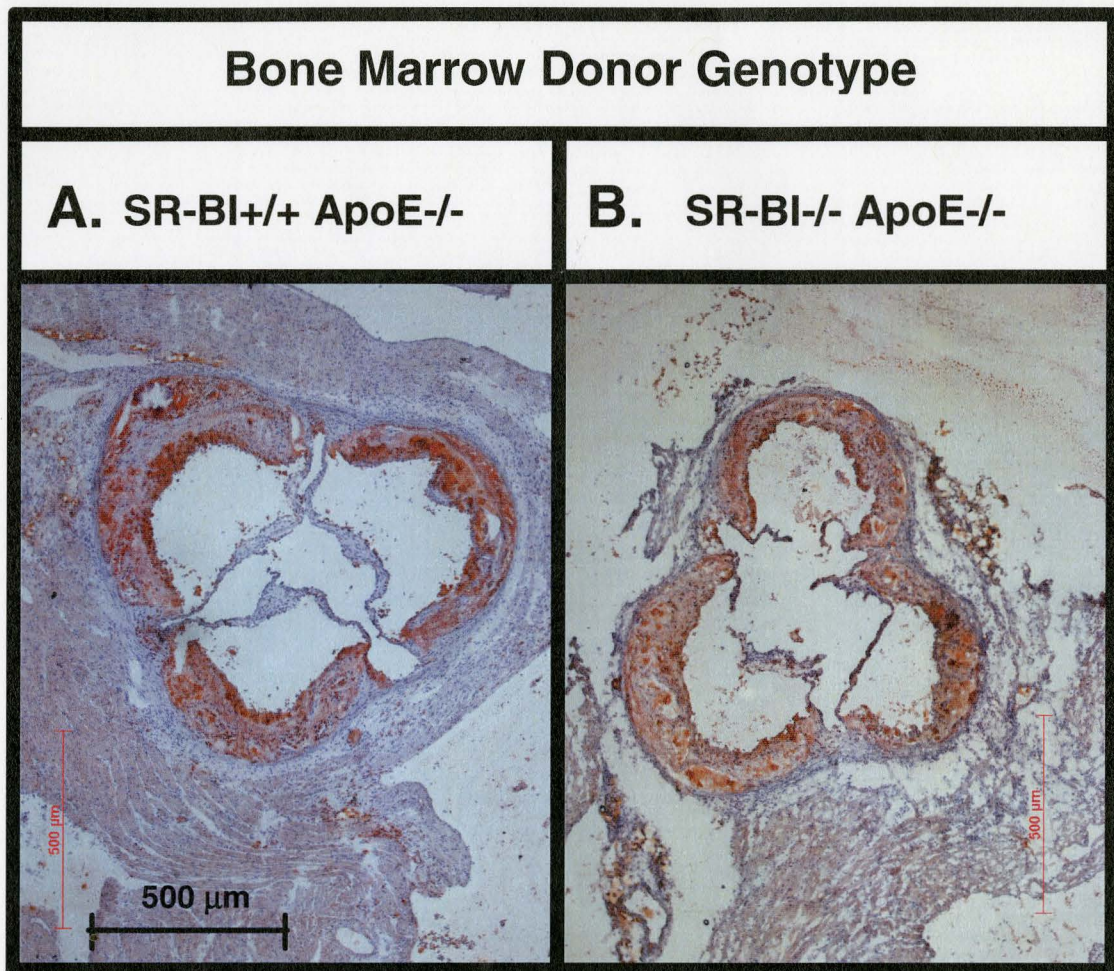


Figure 14. Histological analysis of atherosclerotic plaque in the aortic roots of bone marrow transplanted mice. Atherosclerosis in aortas from mice transplanted with either control SR-BI+/+ ApoE-/- (A) or SR-BI-/- ApoE-/- (B) bone marrow was visualized by Oil Red O staining of cross sections from aortic roots in the hearts of mice. One month after transplantation, mice were fed an atherogenic, high fat western type diet for 12 weeks (*Materials and Methods*, 2.2.6. *Induction of Atherosclerosis*). Mice were euthanized and hearts were harvested and frozen in embedding medium. Hearts were then sectioned, with cross sections collected on glass slides and stained for lipid-rich atherosclerotic plaque with Oil Red O (*Materials and Methods*, 2.2.10 *Tissue Collection and Morphometric Analysis of Aortas and Aortic Sinus*). Images were captured using a Zeiss Axiovert 200M inverted microscope, and the extent of atherosclerosis was determined morphometrically using Axiovision 3.1 software as the total area of lipid-rich Oil Red O stained plaque for each section. Scale bars correspond to 500 μm .

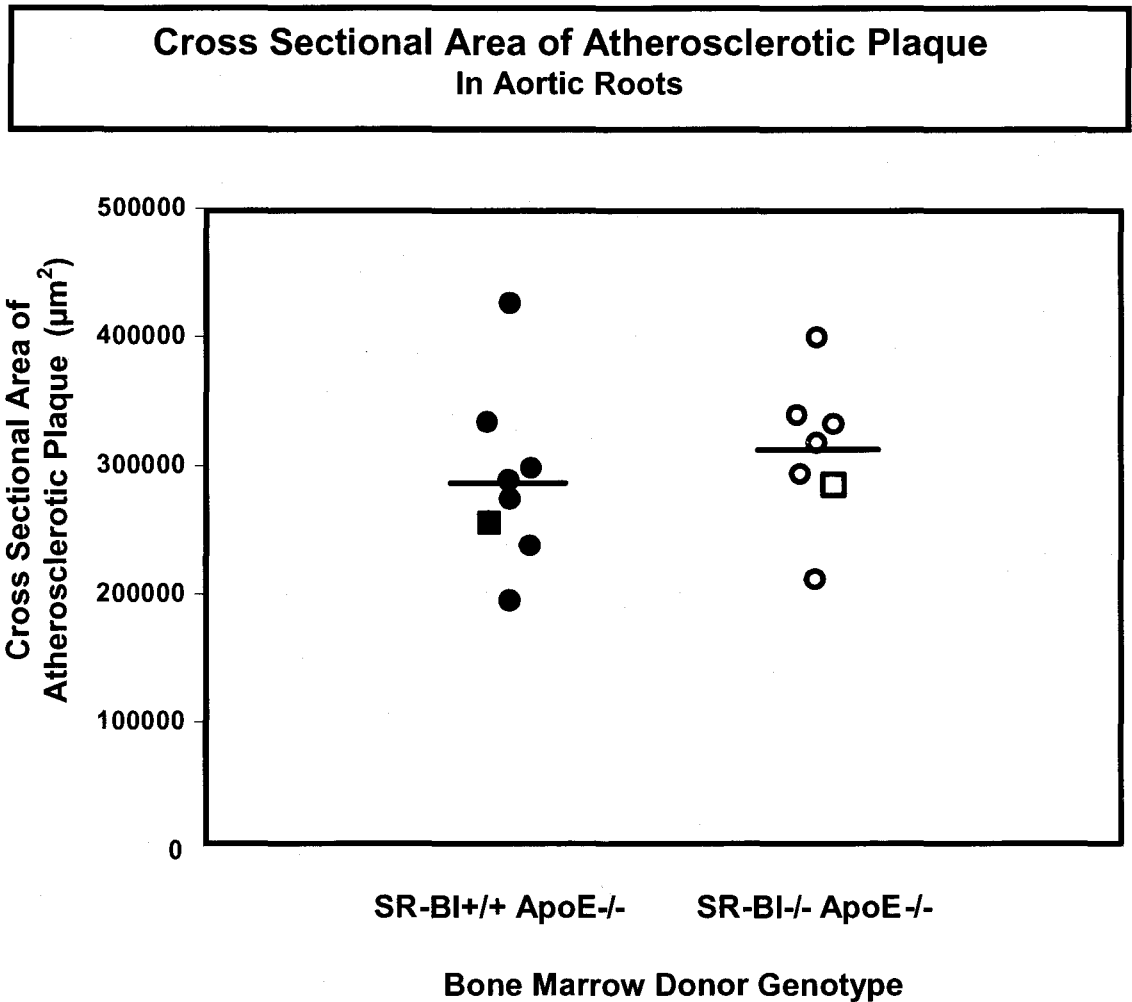


Figure 15. Cross sectional area of atherosclerotic plaque in the aortic roots from ApoE^{-/-} mice transplanted with bone marrow from either SR-BI^{+/+} ApoE^{-/-} (closed circles) or SR-BI^{-/-} ApoE^{-/-} (open circles) bone marrow. Histological analysis of atherosclerotic plaque in the aortic root was carried out as described in the legend to Figure 14. The cross sectional area of atherosclerotic plaque was determined morphometrically using Axiovision 3.1 software. Values corresponding to individual mice are plotted. The mean cross sectional areas are indicated by the horizontal bars and correspond to $288123 \pm 69235 \mu\text{m}^2$ for mice receiving SR-BI^{+/+} ApoE^{-/-} bone marrow, and $310628 \pm 57580 \mu\text{m}^2$ for mice receiving SR-BI^{-/-} ApoE^{-/-} bone marrow. The square symbols correspond to the sections shown in Figure 14. No statistically significant difference was seen in atherosclerosis in the aortic roots of mice in the two groups ($p=0.25$).

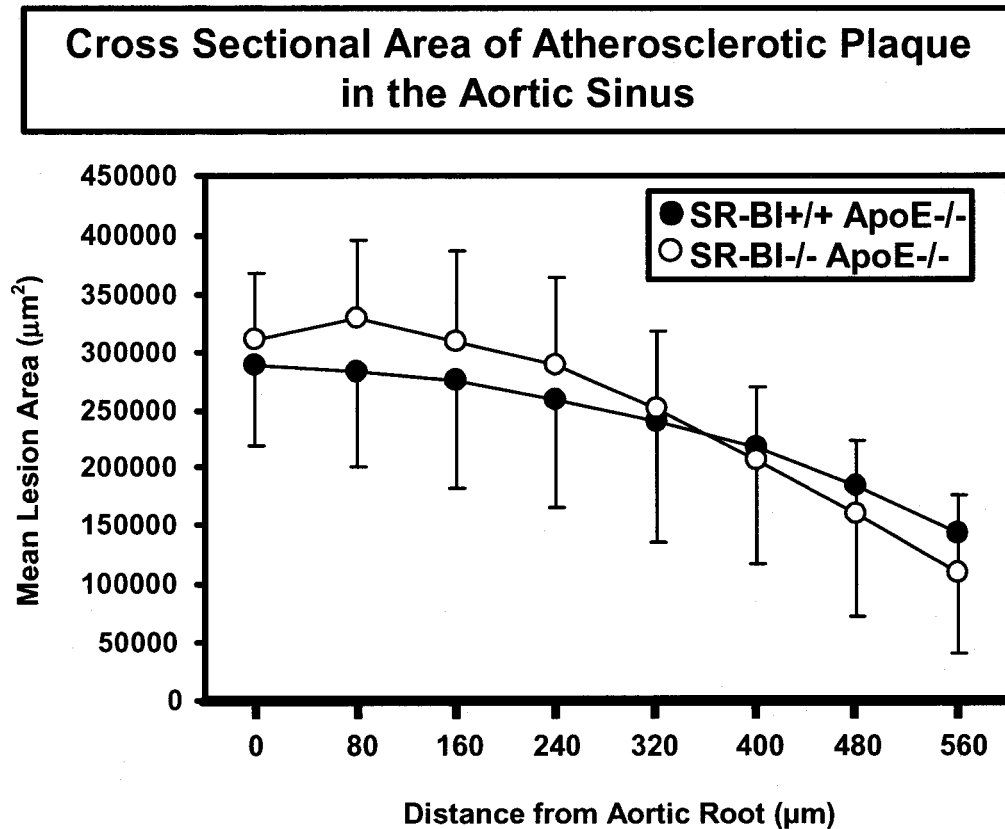


Figure 16. Cross sectional area of atherosclerotic plaque in the aortic sinus. Serial cross sections beginning with the aortic root (distance of 0 µm, data point same as that in Figure 15) were collected. Sections spaced at 80 µm intervals were stained with Oil Red O and atherosclerotic plaque cross sectional area was determined as described in the legends to Figures 14 and 15. Cross sectional areas of plaques are plotted vs. the distance from the aortic root for ApoE^{-/-} mice transplanted with either SR-BI^{+/+} ApoE^{-/-} (closed circles, n=8) or SR-BI^{-/-} ApoE^{-/-} (open circles, n=7) bone marrow. Values shown are the means ± SD in µm². No significant difference was found for any section level between the two groups (p>0.05).

3.5 Effects of Selective Lack of SR-BI in Bone Marrow Derived Cells on Lipoprotein and Cholesterol Metabolism and Atherosclerosis in ApoE ^{-/-} Mice

To summarize, mice transplanted with SR-BI ^{-/-} ApoE ^{-/-} bone marrow showed no significant changes in plasma total cholesterol, or cholesterol associated with VLDL-sized or IDL/LDL-sized lipoproteins compared to control mice transplanted with SR-BI ^{+/+} ApoE ^{-/-} bone marrow. However, they did show significantly lower levels of cholesterol associated with HDL-sized particles compared to controls. Mice transplanted with SR-BI ^{-/-} ApoE ^{-/-} bone marrow showed significantly increased atherosclerotic plaque development than controls in the abdominal aorta but not in the thoracic aorta or the aortic sinus.

4. Discussion

4.1 Potential Mechanisms by which SR-BI may Protect Against Atherosclerosis

Collective data from studies in mice with normal, overexpressed, attenuated, or absent SR-BI expression on various genetic backgrounds suggest that SR-BI has a significant role in HDL and possibly non-HDL cholesterol clearance, and in protection against atherosclerosis (*Introduction*, Table 1). SR-BI/LDL receptor double knockout mice fed a high fat diet exhibit a 515% increase in atherosclerosis compared to LDL receptor single knockout controls, and SR-BI^{att}/LDLR knockout mice exhibit a 69% to 171% increase in atherosclerosis compared to controls [Covey SD *et al*, 2003; Huszar D *et al*, 2000]. Deletion of SR-BI in ApoE knockout mice also results in dramatic acceleration of atherosclerosis development, in addition to a variety of abnormalities in other physiologic systems [Braun A *et al*, 2002].

Based on these and additional *in vivo* and *in vitro* studies, there are several mechanisms involving SR-BI that can potentially be responsible for its anti-atherogenic effect. First, as seen from studies testing the effects of hepatic overexpression of SR-BI, a significant proportion of this protection against atherosclerosis involves SR-BI mediated cholesterol clearance in the liver, evidenced by increased hepatic uptake and biliary secretion of HDL cholesterol, thus playing an important role in reverse cholesterol transport [Kozarsky KF *et al*, 1997; Ueda Y *et al*, 1999; Wang N *et al*, 1998].

Second, it has been seen in cell culture studies that SR-BI can promote HDL-mediated cholesterol efflux [Gi Y *et al*, 1997; Rothblat G *et al*, 1999]. Also, SR-BI deletion in bone marrow derived macrophage foam cells results in increased atherosclerosis [Covey SD, 2003]. This suggests that SR-BI in macrophage foam cells may mediate cholesterol efflux to HDL, thus contributing to anti-atherogenicity.

Furthermore, SR-BI deletion in ApoE knockout mice results in increased levels of pro-atherogenic lipoproteins such as VLDL, LDL, or abnormally large HDL-like particles, with loss of normal anti-atherogenic HDL particles [Trigatti B *et al*, 1999]. This suggests that SR-BI prevents the accumulation of pro-atherogenic lipoproteins in plasma, thus contributing to lower risk for atherosclerosis.

SR-BI can also protect against atherosclerosis by its influence on nitric oxide synthase activation. Nitric oxide in the vessel endothelium has been shown to have atheroprotective functions [Napoli C *et al*, 2001], and activation of endothelial nitric oxide synthase can be promoted by HDL binding to SR-BI [Yuhanna IS *et al*, 2001].

Finally, in both SR-BI/ApoE double knockout mice and SR-BI/LDL receptor double knockout mice, erythrocyte morphology is seen to be significantly affected relative to respective controls. Erythrocytes in these mice exhibit macrocytosis, irregular shape, and large autophagosomes, properties characteristic of intermediates in reticulocytosis [Krieger M, 2001; Holm TM *et al*, 2002; Covey *et al*, 2003]. The resulting macrocytic anemia leads to hypoxia, which is thought to have a part in the promotion of atherosclerosis [Gainer JL, 1987]. In light of these observations, it appears that SR-BI

may have a role in the maintenance of normal erythrocyte morphology, a potential component of its anti-atherogenic role.

4.2 Effects of SR-BI Deletion in Bone Marrow Derived Cells on Lipoprotein Metabolism in ApoE Knockout Mice

SR-BI deletion in bone marrow derived cells was achieved by the generation of chimeric mice via bone marrow transplantation [Linton MF, 1995; Covey SD *et al*, 2003]. No difference was seen in total cholesterol levels between the experimental and control groups before or after being placed on a high fat diet, and as expected, total cholesterol levels were increased in plasma collected from animals after 3 months of being fed the high fat diet (four months after transplantation) compared to levels before administration of the high fat diet. Preliminary data from 3 mice transplanted with either SR-BI $-/-$ ApoE $-/-$ (2 mice) or SR-BI $+/+$ ApoE $-/-$ (1 mouse) bone marrow that were maintained on normal chow for the 4 month period following transplantation showed total cholesterol levels similar to those seen in mice on normal chow for one month after transplantation, prior to being placed on a high fat diet.

The lack of differences between total cholesterol levels in the two groups was expected in light of findings that hepatic SR-BI plays the major role in lipoprotein and cholesterol metabolism [Kozarsky KF *et al*, 1997; Ueda Y *et al*, 1999; Mardones P *et al*, 2001], with little contribution from SR-BI in macrophages and other bone marrow derived cells.

When levels of cholesterol associated with VLDL- and IDL/LDL-sized lipoproteins were analyzed, no difference was seen in the two groups of mice. However, cholesterol associated with HDL-sized lipoproteins was seen to be decreased in mice transplanted with SR-BI $-/-$ ApoE $-/-$ bone marrow compared to control mice transplanted with SR-BI $+/+$ ApoE $-/-$ bone marrow. This is in contrast to the findings of Covey *et al*, where no differences in HDL-associated cholesterol were seen in LDL receptor $-/-$ mice transplanted with either SR-BI $+/+$ or SR-BI $-/-$ bone marrow [Covey SD *et al*, 2003]. Also, similar transplantation studies in ApoE and LDL receptor knockout mice fed a high fat diet transplanted with bone marrow cells lacking ABCA1, a protein mediating cholesterol efflux to ApoAI, showed an increase in atherosclerosis without any significant change in total cholesterol levels or lipoprotein profiles [Aiello R *et al*, 2002]. In the preliminary set of 3 mice (mentioned above), no differences were seen in levels of total cholesterol or VLDL-, LDL-, or HDL-associated cholesterol between the samples from three mice transplanted with either SR-BI $+/+$ ApoE $-/-$ or SR-BI $-/-$ ApoE $-/-$ bone marrow.

Levels of cholesterol associated with HDL-sized lipoproteins accounted for about 2-3% of total cholesterol in transplanted ApoE knockout mice fed a high fat diet. One reason for lower HDL cholesterol levels in mice transplanted with SR-BI $-/-$ ApoE $-/-$ bone marrow may be that the lack of SR-BI in macrophages results in decreased efflux of cholesterol from macrophages to HDL. However, SR-BI mediated efflux to HDL may occur from non-bone marrow derived cells in a variety of other tissues where SR-BI is expressed; moreover, selective SR-BI deletion in macrophages of LDL receptor knockout

mice does not result in decreased HDL-sized lipoprotein cholesterol levels compared to controls [Covey SD *et al*, 2003]. No study to date has been carried out on LDL receptor knockout mice transplanted with SR-BI *-/-* LDL receptor *-/-* bone marrow. Since ApoE was also absent in macrophages of mice in the control group, it is likely that this difference may be the result of the combined absence of SR-BI and ApoE in bone marrow derived cells used in this experiment. Mice lacking both SR-BI and ApoE show dramatically accelerated atherosclerosis development, myocardial dysfunction, and premature death on normal chow [Braun A *et al*, 2002] compared to mice deficient in both SR-BI and the LDLR receptor, which develop diet-induced atherosclerosis in the absence of severe symptoms seen in the SR-BI/ApoE double knockout mouse [Covey SD *et al*, 2003]. Selective uptake is seen to be decreased in ApoE knockout mice [Arai T *et al*, 1999], implying that ApoE deficiency may have an influence on SR-BI and its interaction with HDL. Taken together, these findings point to the possibility that the absence of ApoE with SR-BI in the macrophages of mice in our study is associated with the resulting discrepancy in HDL cholesterol levels between the experimental and control mouse groups.

To investigate this further, the same study can be conducted for ApoE *-/-* recipients transplanted with either SR-BI *+/+* or SR-BI *-/-* donor bone marrow and normal expression of the ApoE gene in bone marrow derived cells, as done in LDLR knockout mice by Covey *et al* [Covey SD *et al*, 2003]. Also, cell culture studies to look at cholesterol efflux for cells carrying the SR-BI *+/+*, SR-BI *-/-*, ApoE *-/-*, and SR-BI *-/-* ApoE *-/-* genotypes can be carried out to assess differences in efflux patterns for SR-BI

and ApoE deficiency independently as well as combined SR-BI/ApoE deficiency. This would aid in the understanding of possible underlying mechanisms behind our results.

4.3 Effects of SR-BI Deletion in Bone Marrow Derived Cells on Atherosclerosis in ApoE Knockout Mice

Analysis of aortas revealed 1.3-fold increased atherosclerosis in fat-fed ApoE $-/-$ mice that received SR-BI $-/-$ ApoE $-/-$ bone marrow compared to those that received SR-BI $+/+$ ApoE $-/-$ bone marrow. This difference is due to an approximately 2.5-fold increase in atherosclerosis in the abdominal aortas of mice from the experimental group. Assays for atherosclerosis development in the proximal aorta (% plaque coverage in thoracic aorta) and the aortic sinus (plaque thickness lesion area) showed no significant differences between the two groups. It was thus seen that along with increased atherosclerosis, macrophage specific SR-BI deletion in ApoE knockout mice results in redistribution of plaque in the aorta.

Our recipient mice were three months of age at the time of transplantation. ApoE knockout mice develop detectable atherosclerosis spontaneously by about 3-5 months of age [Nakashima Y *et al*, 1994; Reddick RL *et al*, 1994]. As mentioned (*Introduction, 1.1 Atherosclerosis and Plasma Cholesterol*), macrophages play an important role in the early stages of atherosclerotic development. If macrophage SR-BI is athero-protective by way of mediating cholesterol efflux to HDL, it is likely that it would have a more active

role during the initiation of new plaque formation, a potential explanation for the redistribution of plaque seen in ApoE knockout mice transplanted with SR-BI *-/-* ApoE *-/-* bone marrow.

The combined results of increased atherosclerosis with plaque redistribution were also seen in the study conducted by Covey *et al* on LDL receptor knockout mice in our laboratory fed a high fat diet for 4 months; increased atherosclerosis was seen in the aortas of mice that received bone marrow cells lacking SR-BI relative to controls, with an almost two-fold increase in atherosclerosis in the aortic arches [Covey SD *et al*, 2003; Covey SD, Doctoral Thesis, 2003], but without a significant difference in the descending aorta.

The finding of increased atherosclerosis with macrophage-specific SR-BI deletion in ApoE *-/-* mice, and in LDL receptor *-/-* mice [Covey SD *et al*, 2003], is consistent with the effects of macrophage-specific deletion of ABCA1, which mediates cholesterol efflux from macrophages to ApoAI, in ApoE or LDL receptor knockout mice [Aiello R *et al*, 2002; van Eck M *et al*, 2002]. This points to the possibility that SR-BI in bone marrow derived cells, like ABCA1, may confer its anti-atherogenic effect by way of its role in cholesterol efflux from macrophage foam cells.

In conclusion, it is seen from the data that SR-BI in bone marrow derived cells contributes to the overall athero-protective role of SR-BI. As mentioned, hepatic expression of SR-BI has a larger influence on anti-atherogenicity via selective cholesterol uptake [Kozarsky KF *et al*, 1997; Ueda Y *et al*, 1999; Mardones P *et al*, 2001], but SR-BI in bone marrow derived cells presumably confers this effect via cholesterol efflux to

HDL. We have demonstrated that SR-BI in bone marrow derived cells can make a contribution to the overall atheroprotective role of SR-BI. Therefore, stimulation of SR-BI expression in these cells may constitute an effective strategy in the treatment of human atherosclerosis.

Note: Zhang W *et al* [2003] reported very recently that inactivation of macrophage SR-BI in ApoE deficient mice results in increased atherosclerotic lesion development. In this study, ApoE *-/-* recipient mice were transplanted with either SR-BI *+/+* ApoE *-/-* or SR-BI *-/-* ApoE *-/-* bone marrow and fed a normal chow diet for 12 weeks after transplantation. Atherosclerosis was seen to be increased in the group transplanted with SR-BI *-/-* ApoE *-/-* bone marrow with no differences in total cholesterol levels, lipoprotein distribution, or HDL levels in the two groups. These results are consistent with our finding increased atherosclerosis in ApoE *-/-* mice lacking macrophage SR-BI and also with our preliminary results from three mice (mentioned above), which showed no differences in total cholesterol levels, lipoprotein distribution, or HDL cholesterol levels [Zhang W *et al*, 2003].

5. References

- Acton SL, Sherer PE, Lodish HF, Krieger M: **Expression cloning of SR-BI, a CD36-related class B scavenger receptor.** *J Biol Chem.* 1994, 269(33):21003-9.
- Acton S, Rigotti A, Landshulz KT, Xu S, Hobbs HH, Krieger M: **Identification of scavenger receptor SR -BI as a high density lipoprotein receptor.** *Science.* 1996, 271(5248):518-20.
- Aiello, R *et al*: **Increased Atherosclerosis in Hyperlipidemic Mice With Inactivation of ABCA1 in Macrophages.** *Arterioscler Thromb Vasc Biol.* 2002, 22:630-637.
- Allain CC, Poon LS, Chan CS, Richmond W, Fu PC: **Enzymatic determination of total serum cholesterol.** *Clin Chem.* 1974, 20(4):470-5.
- Arai T, Rinninger F, Varban L, Fairchild-Huntress V, Liang CP, Chen W, Seo T, Deckelbaum R, Huszar D, Tall AR: **Decreased selective uptake of high density lipoprotein cholesteryl esters in apolipoprotein E knock-out mice.** *Proc Natl Acad Sci U S A.* 1999, 96(21):12050-5.
- Arai T, Wang N, Bezouevski M, Welch C, Tall AR: **Decreased atherosclerosis in heterozygous low density lipoprotein receptor-deficient mice expressing the scavenger receptor BI transgene.** *J Biol Chem.* 1999, 274(4):2366-71.
- Barter PJ, Brewer HB Jr, Chapman MJ, Hennekens CH, Rader DJ, Tall AR: **Cholesteryl ester transfer protein: a novel target for raising HDL and inhibiting atherosclerosis.** *Arterioscler Thromb Vasc Biol.* 2003, 23(2):160-7. Review.
- Basso F, Freeman L, Knapper CL, Remaley A, Stonik J, Neufeld EB, Tansey T, Amar MJ, Fruchart-Najib J, Duverger N, Santamarina-Fojo S, Brewer HB Jr: **Role of the hepatic ABCA1 transporter in modulating intrahepatic cholesterol and plasma HDL cholesterol concentrations.** *J. Lipid Res.* 2003, 44:296-302.
- Bonnefont-Rousselot D, Therond P, Beaudeux JL, Peynet J, Legrand A, Delattre J: **High density lipoproteins (HDL) and the oxidative hypothesis of atherosclerosis.** *Clin Chem Lab Med.* 1999, 37(10):939-48. Review.
- Braun A, Trigatti BL, Post MJ, Sato K, Simons M, Edelberg JM, Rosenberg RD, Schrenzel M, Krieger M: **Loss of SR-BI Expression Leads to the Early Onset of Occlusive Atherosclerotic Coronary Artery Disease, Spontaneous Myocardial Infarctions, Severe Cardiac Dysfunction, and Premature Death in Apolipoprotein E-Deficient Mice.** *Circ Res* 2002, 90:270-276.

Braun A, Zhang S, Miettinen HE, Ebrahim S, Holm TM, Vasile E, Post MJ, Yoerger DM, Picard MH, Krieger JL, Andrews NC, Simons M, Krieger M: **Probucol prevents early coronary heart disease and death in the high-density lipoprotein receptor SR - BI/apolipoprotein E double knockout mouse.** *Proc. Natl. Acad. Sci.* 2003, 100(12):7283-7288.

Breslow JL: **Mouse models of atherosclerosis.** *Science.* 1996, 272(5262):685-8. Review.

Brown MS, Goldstein JL: **Lipoprotein metabolism in the macrophage: implications for cholesterol deposition in atherosclerosis.** *Annu Rev Biochem.* 1983, 52:223-61. Review.

Calara F, Silvestre M, Casanada F, Yuan N, Napoli C, Palinski W: **Spontaneous plaque rupture and secondary thrombosis in apolipoprotein E-deficient and LDL receptor-deficient mice.** *J Pathol.* 2001, 195(2):257-63.

Callow MJ, Verstuyft J, Tangirala R, Palinski W, Rubin EM: **Atherogenesis in transgenic mice with human apolipoprotein B and lipoprotein (a).** *J Clin Invest.* 1995, 96(3):1639-46.

Calvo D, Gomez-Coronado D, Suarez Y, Lasuncion MA, Vega MA: **Human CD36 is a high affinity receptor for the native lipoproteins HDL, LDL, and VLDL.** *J Lipid Res.* 1998, 39(4):777-88.

Claudiel T, Leibowitz MD, Fievet C, Tailleux A, Wagner B, Repa JJ, Torpier G, Lobaccaro JM, Paterniti JR, Mangelsdorf DJ, Heymen RA, Auwerx J: **Reduction of atherosclerosis in apolipoprotein E knockout mice by activation of the retinoid X receptor.** *Proc Natl Acad Sci U S A.* 2001, 98(5):2610-5.

Connelly MA, De La Llera-Moya M, Peng Y, Drazul-Schrader D, Rothblat GH, Williams DL: **Separation of Lipid Transport Functions by Mutations in the Extracellular Domain of Scavenger Receptor Class B, Type I.** *J. Biol. Chem.* 2003, 278(28):25773-782.

Covey SD, Krieger M, Wang W, Penman M, Trigatti BL: **Scavenger Receptor Class B Type I-Mediated Protection Against Atherosclerosis in LDL Receptor-Negative Mice Involves Its Expression in Bone Marrow-Derived Cells.** *Arterioscler Thromb Vasc Biol.* 2003, 23(9):1589-94.

Dansky HM, Charlton SA, Sikes JL, Heath SC, Simantov R, Levin LF, Shu P, Moore KJ, Breslow JL, Smith JD: **Genetic background determines the extent of atherosclerosis in ApoE-deficient mice.** *Arterioscler Thromb Vasc Biol.* 1999, 19(8):1960-8.

Davis HR Jr, Compton DS, Hoos L, Tetzloff G: **Ezetimibe, a potent cholesterol absorption inhibitor, inhibits the development of atherosclerosis in ApoE knockout mice.** *Arterioscler Thromb Vasc Biol.* 2001, 21(12):2032-8.

de la Llera-Moya M, Rothblat GH, Connelly MA, Kellner Weibel G, Sakr SW, Phillips MC, Williams DL: **Scavenger receptor BI (SR-BI) mediates free cholesterol flux independently of HDL tethering to the cell surface.** *J Lipid Res.* 1999, 40(3):575-80.

de Villiers WJ, Smart EJ: **Macrophage scavenger receptors and foam cell formation.** *J Leukoc Biol.* 1999, 66(5):740-6. Review.

Fazio S, Babaev VR, Murray AB, Hasty AH, Carter KJ, Gleaves LA, Atkinson JB, Linton MF: **Increased atherosclerosis in mice reconstituted with apolipoprotein E null macrophages.** *Proc Natl Acad Sci U S A.* 1997, 94(9):4647-52.

Fazio S, Linton MF: **Mouse models of hyperlipidemia and atherosclerosis.** *Front Biosci.* 2001, 6: D515-25. Review.

Fazio S, Babaev VR, Burleigh ME, Major AS, Hasty AH, Linton MF: **Physiological expression of macrophage apoE in the artery wall reduces atherosclerosis in severely hyperlipidemic mice.** *J. Lipid Res.* 2002, 43:1602-1609.

Gainer JL **Hypoxia and atherosclerosis: re-evaluation of an old hypothesis.** *Atherosclerosis.* 1987, 68(3):263-6.

Glass C, Pittman RC, Weinstein DB, Steinberg D: **Dissociation of tissue uptake of cholesterol ester from that of apoprotein A-I of rat plasma high density lipoprotein: selective delivery of cholesterol ester to liver, adrenal, and gonad.** *Proc Natl Acad Sci U S A.* 1983, 80(17):5435-9.

Goldstein JL, Brown MS: **The LDL receptor and the regulation of cellular cholesterol metabolism.** *J Cell Sci Suppl.* 1985, 3:131-7. Review.

Gotto AM Jr: **Lipoprotein metabolism and the etiology of hyperlipidemia.** *Hosp Pract (Off Ed).* 1988, Suppl 1:4-13. Review.

Gordon T, Castelli WP, Hjortland MC, Kannel WB, Dawber TR: **High density lipoprotein as a protective factor against coronary heart disease. The Framingham Study.** *Am J Med.* 1977, 62(5):707-14.

Gu X, Trigatti B, Xu S, Acton S, Babitt J, Krieger M: **The Efficient Cellular Uptake of High Density Lipoprotein Lipids via Scavenger Receptor Class B Type I Requires Not Only Receptor-mediated Surface Binding but Also Receptor-specific Lipid**

Transfer Mediated by Its Extracellular Domain. *J Biol Chem.* 1998, 273(41):26338-26348.

Gu X, Kozarsky K, Krieger M: **Scavenger receptor class B, type I-mediated [3H]cholesterol efflux to high and low density lipoproteins is dependent on lipoprotein binding to the receptor.** *J Biol Chem.* 2000, 275(39):29993-30001.

Hauser H, Dyer JH, Nandy A, Vega MA, Werder M, Bieliauskaite E, Weber FE, Compassi S, Gemperli A, Boffelli D, Wehrli E, Schulthess G, Phillips MC: **Identification of a receptor mediating absorption of dietary cholesterol in the intestine.** *Biochemistry.* 1998, 37(51):17843-50.

Herijgers N, Van Eck M, Groot PH, Hoogerbrugge PM, Van Berkel TJ: **Effect of bone marrow transplantation on lipoprotein metabolism and atherosclerosis in LDL receptor-knockout mice.** *Arterioscler Thromb Vasc Biol.* 1997, 17(10):1995-2003.

Holm TM, Braun A, Trigatti BL, Brugnara C, Sakamoto M, Krieger M, Andrews NC: **Failure of red blood cell maturation in mice with defects in the high-density lipoprotein receptor SR-BI.** *Blood.* 2002, 99(5):1817-24.

Huszar D, Varban ML, Rinninger F, Feeley R, Arai T, Fairchild-Huntress V, Donovan MJ, Tall AR: **Increased LDL cholesterol and atherosclerosis in LDL receptor-deficient mice with attenuated expression of scavenger receptor B1.** *Arterioscler Thromb Vasc Biol.* 2000, 20(4):1068-73.

Ishibashi S, Brown MS, Goldstein JL, Gerard RD, Hammer RE, Herz J: **Hypercholesterolemia in low density lipoprotein receptor knockout mice and its reversal by adenovirus-mediated gene delivery.** *J Clin Invest.* 1993, 92(2):883-93.

Ji Y, Jian B, Wang N, Sun Y, Moya ML, Phillips MC, Rothblat GH, Swaney JB, Tall AR: **Scavenger receptor BI promotes high density lipoprotein-mediated cellular cholesterol efflux.** *J Biol Chem.* 1997, 272(34):20982-5.

Ji Y, Wang N, Ramakrishnan R, Sehayek E, Huszar D, Breslow JL, Tall AR: **Hepatic scavenger receptor BI promotes rapid clearance of high density lipoprotein free cholesterol and its transport into bile.** *J Biol Chem.* 1999, 274(47):33398-402.

Jian B, de al Llera-Moya M, Ji Y, Wang N, Phillips MC, Swaney JB, Tall AR, Rothblat GH: **Scavenger receptor class B type I as a mediator of cellular cholesterol efflux to lipoproteins and phospholipid acceptors.** *J Biol Chem.* 1998, 273(10):5599-606.

- Kozarsky KF, Donahee MH, Rigotti A, Iqbal SN, Edelman ER, Krieger M: **Overexpression of the HDL receptor SR-BI alters plasma HDL and bile cholesterol levels.** *Nature.* 1997, 387(6631):414-7.
- Kozarsky KF, Donahee MH, Glick JM, Krieger M, Rader DJ: **Gene transfer and hepatic overexpression of the HDL receptor SR-BI reduces atherosclerosis in the cholesterol-fed LDL receptor-deficient mouse.** *Arterioscler Thromb Vasc Biol.* 2000, 20:721-7.
- Krieger M: **The “best” of cholesterol, the “worst” of cholesterol: a tale of two receptors.** *Proc Natl Acad Sci U.S.A.* 1998, 95(8):4077-80. Review.
- Krieger, M: **Scavenger receptor class B type I is a multiligand HDL receptor that influences diverse physiologic systems.** *J. Clin Invest.* 2001, 108:793-797. Review.
- Kwiterovich PO Jr: **The anti-atherogenic role of high density lipoprotein cholesterol.** *Am J Cardiol.* 1998, 82(9A):13Q-21Q. Review.
- La Rosa JC: **Understanding risk in hypercholesterolemia.** *Clin Cardiol.* 2003, 26(1 Suppl 1):13-6.
- Laird PW, Zijderveld A, Linders K, Rudnicki MA, Jaenisch R, Berns A: **Simplified mammalian DNA isolation procedure.** *Nucleic Acids Res.* 1991, 19(15):4293.
- Lambert G, Chase MB, Dugi K, Bensadoun A, Brewer HB Jr, Santamarina-Fojo S: **Hepatic lipase promotes the selective uptake of high density lipoprotein-cholesteryl esters via the scavenger receptor B1.** *J Lipid Res.* 1999, 40(7):1294-303.
- Layne MD, Patel A, Chen YH, Rebel VI, Carvajal IM, Pellacani A, Ith B, Zhao D, Schreiber BM, Yet SF, Lee ME, Storch J, Perrella MA: **Role of macrophage-expressed adipocyte fatty acid binding protein in the development of accelerated atherosclerosis in hypercholesterolemic mice.** *FASEB J.* 2001, 15(14):2733-5.
- Libby P: **Managing the risk of atherosclerosis: the role of high-density lipoprotein.** *Am J Cardiol.* 2001, 88(12A):3N-8N.
- Libby P: **Vascular biology of atherosclerosis: overview and state of the art.** *Am J Cardiol.* 2003, 9(3A):3A-6A.
- Linton MF, Fazio S: **Macrophages, lipoprotein metabolism, and atherosclerosis: insights from murine bone marrow transplantation studies.** *Curr Opin Lipidol.* 1999, 10(2):97-105. Review.

Mahley RW: **Development of accelerated atherosclerosis. Concepts derived from cell biology and animal model studies.** *Arch Pathol Lab Med.* 1983,107(8):393-9. Review.

Makowski L, Boord JB, Maeda K, Babaev VR, Uysal KT, Morgan MA, Parker RA, Suttles J, Fazio S, Hotamisligil GS, Linton MF: **Lack of macrophage fatty-acid-binding protein aP2 protects mice deficient in apolipoprotein E against atherosclerosis.** *Nat Med.* 2001, 7(6):699-705.

Mardones P, Quinones V, Amigo L, Moreno M, Miguel JF, Schwarz M, Miettinen HE, Trigatti B, Krieger M, VanPatten S, Cohen DE, Rigotti A: **Hepatic cholesterol and bile acid metabolism and intestinal cholesterol absorption in scavenger receptor class B type I-deficient mice.** *J. Lip. Res.* 2001, 42:170-180.

Mardones P, Strobel P, Miranda S, Leighton F, Quinones V, Amigo L, Rozowski J, Krieger M, Rigotti A: **Alpha-tocopherol metabolism is abnormal in scavenger receptor class B type I (SR-BI)-deficient mice.** *J Nutr.* 2002, 132(3):443-9.

Miettinen H, Rayburn H, Krieger M: **Abnormal lipoprotein metabolism and reversible female infertility in HDL receptor (SR -BI)-deficient mice.** *J. Clin. Invest.* 2001, 108:1717-1722.

Nakashima Y, Plump AS, Raines EW, Breslow JL, Ross R: **ApoE-deficient mice develop lesions of all phases of atherosclerosis throughout the arterial tree.** *Arterioscler Thromb.* 1994, 14(1):133-40.

Napoli C, Ignarro LJ: **Nitric oxide and atherosclerosis.** *Nitric Oxide.* 2001, 5(2):88-97. Review.

Newton RS, Krause BR: **HDL therapy for the acute treatment of atherosclerosis.** *Atheroscler Suppl.* 2002, 3:31-38.

Nofer JR, Kehrel B, Fobker M, Levkau B, Assmann G, von Eckardstein A: **HDL and arteriosclerosis: beyond reverse cholesterol transport.** *Atherosclerosis.* 2002, 161(1):1-16. Review.

Paigen B, Morrow A, Holmes PA, Mitchell D, Williams RA: **Quantitative assessment of atherosclerotic lesions in mice.** *Atherosclerosis.* 1987, 68(3):231-40.

Plump AS, Smith JD, Hayek T, Aalto-Setälä K, Walsh A, Verstuyft JG, Rubin EM, Breslow JL: **Severe hypercholesterolemia and atherosclerosis in apolipoprotein E-deficient mice created by homologous recombination in ES cells.** *Cell.* 1992, 69:71(2):343-53.

Purcell-Huynh DA, Farese RV Jr, Johnson DF, Flynn LM, Pierotti V, Newland DL, Linton MF, Sanan DA, Young SG: **Transgenic mice expressing high levels of human apolipoprotein B develop severe atherosclerotic lesions in response to a high-fat diet.** *J Clin Invest.* 1995, 95(5):2246-57.

Reddick RL, Zhang SH, Maeda N: **Atherosclerosis in mice lacking apo E. Evaluation of lesion development and progression.** *Arterioscler Thromb.* 1994, 14(1):141-7; Erratum in: *Arterioscler Thromb* 1994, 14(5):839.

Rigotti A, Acton SL, Krieger M: **The class B scavenger receptors SR-BI and CD36 are receptors for anionic phospholipids.** *J Biol Chem.* 1995, 270(27):16221-4.

Rigotti A, Trigatti BL, Penman M, Rayburn H, Herz J, Krieger M: **A targeted mutation in the murine gene encoding the high density lipoprotein (HDL) receptor scavenger receptor class B type I reveals its key role in HDL metabolism.** *Proc Natl Acad Sci U.S.A.* 1997, 94(23):12610-5.

Rodrigueza WV, Thuahnai ST, Temel RE, Lund-Katz S, Phillips MC, Williams DL: **Mechanism of scavenger receptor class B type I-mediated selective uptake of cholesteryl esters from high density lipoprotein to adrenal cells.** *J Biol Chem.* 1999, 274(29):20344-50.

Roeschlau P, Bernt E, Gruber W: **Enzymatic determination of total cholesterol in serum.** *Z Klin Chem Klin Biochem.* 1974, 12(5):226.

Rothblat GH, de la Llera-Moya M, Atger V, Kellner-Weibel G, Williams DL, Phillips MC: **Cell cholesterol efflux: integration of old and new observations provides new insights.** *J. Lipid Res.* 1999, 40:781-796.

Rothblat GH, de la Llera-Moya M, Favari E, Yancey PG, Kellner-Weibel G: **Cellular cholesterol flux studies: methodological considerations.** *Atherosclerosis.* 2002, 163(1):1-8.

Rust S, Rosier M, Funke H, Real J, Amoura Z, Piette JC, Deleuze JF, Brewer HB, Duverger N, Deneffe P, Assman G: **Tangier disease is caused by mutations in the gene encoding ATP-binding cassette transporter 1.** *Nat Genet.* 1999, 22(4):352-5.

Schwartz CJ, Valente AJ, Sprague EA, Kelley JL, Nerem RM: **The pathogenesis of atherosclerosis: an overview.** *Clin Cardiol.* 1991, 14(2 Suppl 1):11-16. Review.

Sehayek E, Ono JG, Shefer S, Nguyen LB, Wang N, Batta AK, Salen G, Smith JD, Tall AR, Breslow JL: **Biliary cholesterol excretion: a novel mechanism that regulates dietary cholesterol absorption.** *Proc Natl Acad Sci U S A.* 1998, 95(17):10194-9.

- Silver DL, Tall AR: **The cellular biology of scavenger receptor class B type I.** *Curr Opin Lipidol.* 2001, 12(5):497-504. Review.
- Singaraja RR, Brunham LR, Visscher H, Kastelein JJ, Hayden MR: **Efflux and Atherosclerosis: The Clinical and Biochemical Impact of Variations in the ABCA1 Gene.** *Arterioscler Thromb Vasc Biol.* 2003, 23(8):1322-32.
- Sniderman AD, Zhang Z, Genest J, Cianflone K: **Effects on apoB-100 secretion and bile acid synthesis by redirecting cholesterol efflux from HepG2 cells.** *Lipid Res.* 2003, 44(3):527-32.
- Tailleux A, Duriez P, Fruchart JC, Clavey V: **Apolipoprotein A-II, HDL metabolism and atherosclerosis.** *Atherosclerosis.* 2002, 164(1):1-13. Review.
- Tall AR: **An overview of reverse cholesterol transport.** *Eur Heart J.* 1998, 19 Suppl A:A31-5. Review.
- Tangirala RK, Rubin EM, Palinski W: **Quantitation of atherosclerosis in murine models: correlation between lesions in the aortic origin and in the entire aorta, and differences in the extent of lesions between sexes in LDL receptor-deficient and apolipoprotein E-deficient mice.** *J Lipid Res.* 1995, 36(11):2320-8.
- Trigatti B, Rayburn H, Vinals M, Braun A, Miettinen H, Penman M, Hertz M, Schrenzel M, Amigo L, Rigotti A, Krieger M: **Influence of the high density lipoprotein receptor SR-BI on reproductive and cardiovascular pathophysiology.** *Proc Natl Acad Sci U.S.A.* 1999, 96(16):9322-7.
- ^aTrigatti B, Rigotti A, Krieger M: **The role of the high-density lipoprotein receptor SR-BI in cholesterol metabolism.** *Curr Opin Lipidol.* 2000, 11(2):123-31. Review.
- ^bTrigatti BL, Rigotti A, Braun A: **Cellular and physiological roles of SR -BI, a lipoprotein receptor which mediates selective lipid uptake.** *Biochim Biophys Acta.* 2000, 1529(1-3):276-86. Review.
- Tulenko TN, Sumner AE: **The physiology of lipoproteins.** *J Nucl Cardiol.* 2002, 9(6):638-49. Review.
- Ueda Y, Royer L, Gong E, Zhang J, Cooper PN, Francone O, Rubin EM: **Lower Plasma Levels and Accelerated Clearance of High Density Lipoprotein (HDL) and Non-HDL Cholesterol in Scavenger Receptor Class B Type I Transgenic Mice.** *J Biol Chem.* 1999, 274(11):7165-71.

Ueda Y, Gong E, Royer L, Cooper PN, Francone OL, Rubin EM: **Relationship between Expression Levels and Atherogenesis in Scavenger Receptor Class B, Type I Transgenics.** *J Biol Chem.* 2000, 275(27):20368-73.

van Eck M, Bos IS, Kaminski WE, Orso E, Rothe G, Twisk J, Bottcher A, Van Amersfoort ES, Christiansen-Weber TA, Fung-Leung WP, Van Berkel TJ, Schmitz G: **Leukocyte ABCA1 controls susceptibility to atherosclerosis and macrophage recruitment into tissues.** *Proc Natl Acad Sci U S A.* 2002, 99(9):6298-303.

Van Eck M, Twisk J, Hoekstra M, Van Rij BT, Van der Lans CA, Bos IS, Kruijt JK, Kuipers F, Van Berkel TJ: **Differential effects of scavenger receptor BI deficiency on lipid metabolism in cells of the arterial wall and in the liver.** *J. Biol. Chem.* 2003, 278(26):23699-705.

Varban ML, Rinninger F, Wang N, Fairchild-Huntress V, Dunmore JH, Fang Q, Gosselin ML, Dixon KL, Deeds JD, Acton SL, Tall AR, Huszar D: **Targeted mutation reveals a central role for SR-BI in hepatic selective uptake of high density lipoprotein cholesterol.** *Proc Natl Acad Sci U S A.* 1998, 95(8):4619-24.

Veniant M, Withycombe S, Young S: **Lipoprotein Size and Atherosclerosis Susceptibility in Apoe ^{-/-} and Ldlr ^{-/-} Mice.** *Arterioscler Thromb Vasc Biol.* 2001, 21(10):1567-70.

von Eckardstein A, Nofer JR, Assmann G: **High density lipoproteins and arteriosclerosis. Role of cholesterol efflux and reverse cholesterol transport.** *Arterioscler Thromb Vasc Biol.* 2001, 21(1):13-27. Review.

Wang N, Arai T, Ji Y, Rinninger F, Tall AR: **Liver-specific overexpression of scavenger receptor BI decreases levels of very low density lipoprotein ApoB, low density lipoprotein ApoB, and high density lipoprotein in transgenic mice.** *J Biol Chem.* 1998, 273(49):32920-6.

Yamashita S, Sakai N, Nirano K, Ishigami M, Maruyama T, Nakajima N, Matsuzawa Y: **Roles of plasma lipid transfer proteins in reverse cholesterol transport.** *Front Biosci.* 2001, 6:D366-87. Review.

Yuhanna IS, Zhu Y, Cox BE, Hahner LD, Osborne-Lawrence S, Lu P, Marcel YL, Anderson RG, Mendelsohn ME, Hobbs HH, Shaul PW: **High-density lipoprotein binding to scavenger receptor-BI activates endothelial nitric oxide synthase.** *Nat Med.* 2001, 7(7):853-7.

Zhang W, Yancey PG, Su YR, Babaev VR, Zhang Y, Fazio S, Linton MF: **Inactivation of Macrophage Scavenger Receptor Class B Type I Promotes Atherosclerotic Lesion Development in Apolipoprotein E-Deficient Mice.** *Circulation.* 2003, 108:2258-63.